International Journal of Astrophysics and Space Science
2024, Vol. 12, No. 1, pp. 17-36
https://doi.org/10.11648/j.ijass.20241201.12

Research Article

On the Andromeda-Milky Way Future Encounter: Thrice Faster Over Time

Alessandro Trinchera*

Independent Researcher, Stuttgart, Germany

Abstract

This inquiry accurately provides an analytical solution of the orbital free-falling time for the system of galaxies Andromeda-Milky Way within a non-expanding tired-light-dominated framework. The mathematical and physical background involves a two-body problem based on the orbital dynamics in which, in the first scenario, the gravitational interaction between local galaxies dominates over the expanding space. The latter is the standard astrophysical approach undertaken by public fund-based universities all over the world. However, in the second alternative scenario, Andromeda's blueshift has to be corrected for the apparent recession velocity provided by the photon energy loss as a result of multiple interactions between photons and crystallized electrons through the intergalactic medium provided by a Tired Light, specifically, a New Tired Light process. This leads towards a substantial temporal deviation between the classic research approach and this unconventional and independent mindset. Hence, the outcome gives out a disagreement consisting in an orbital free-falling time equal to 1.7 rather than 4.5 billion years. Accordingly, the encounter of the two main galaxies of the Local Group will occur much earlier than estimated thus far. Accordingly, this implies an urgent shift in the scientific mindset as well as a course change in the application of the boundary conditions into forthcoming computational methods.

Keywords

Andromeda-Milky Way Encounter, Orbital Free-Falling Time, Blueshift, Two-Body Problem, Non-Expanding Universe, Photon Energy Loss, New Tired Light

1. Introduction

The ultimate collision between Andromeda Galaxy, so-called Messier 31 or M31, and the Milky Way Galaxy, here abbreviated with MW for simplicity, has attracted the attention of many astrophysicists over the years. Both galaxies are the biggest gravitationally-bound members of the Local Group as shown in Figure 1. We know that when this encounter will happen, it is a sort of travel-through for both galaxies which will most likely end up with a merging process due to gravitation. In this regard, the orbital falling-time concerns the first interaction between the two galaxies in the center-of-mass frame and does not include the successive orbital motion and related time occurring until the galaxies merge together. In this research field, an important factor characterizes the study of this orbital interaction: the blueshift detected. The latter represents the relative radial velocity of M31 along our line of sight which has a negative sign meaning an approach velocity toward the MW. This parameter leads us to forecast mathematically an encounter after a cer-

*Corresponding author: trinchera.ale@gmail.com (Alessandro Trinchera)

Received: 15 October 2024; **Accepted:** 30 October 2024; **Published:** 10 November 2024

tain period of time based on the orbital dynamics. Many inquiries have been carried out regarding the exact value of this velocity. Despite this value was smaller in the past [1], the scientific community reached recently a new reliable value equal to $v_r = -110\ Km/sec$ [2] after necessary corrections. The M31 transverse velocity is also very difficult to estimate. Through the years, different values are reported as for instance $v_t < 200\ Km/sec$ [3] up to a lower value $v_t = 164\ Km/sec$ [4]. However, we will adopt a very important upper-estimation $v_t = 225\ Km/sec$ [5] based on N-body/hydrodynamical simulations of the Local Group dynamics, also in this case corrected for the motion of the Earth-Sun-MW system, which is very useful for our calculation. In our investigation, we remain focused on the analytical solution for the orbital free-falling time in a two-body problem as it is the easiest case to analyze in detail without the influence of other small galaxies within the Local Group and in the vicinity of the pair M31-MW. It would cause the introduction of more factors and several differential equations increasing the complexity of the computation. Indeed, the Triangulum Galaxy or M33 and the Large Magellanic Cloud or LMC might influence the merging process of the pair M31-MW [6] close to 50% probability of delaying the known collision value currently equal to 4.5 billion years up to further some billion years. However, a remaining 50% allow us to postulate the absence of interaction with the rest of galaxies in the Local Group. Another outcome [2] places the M31 satellite galaxy, M33, as direct candidate for the merge to the MW before M31. These results are possible after complex computing simulation within a N-body problem, much more difficult to inquiry analytically like in our case, despite scientists remain constrained within the standard model framework on the contrary to this investigation. We will specifically focus on the orbital dynamics and on the velocities with a unique correction. Astrophysicists exclude any extra correction in the interpretation of the detected Doppler-blueshift of M31. After calculating the free-falling time due to pure gravitational interactions between M31 and the MW, where the expanding space is claimed not play any role in the merging process, we will step into a non-expanding framework based on which the blueshift of Andromeda has to be corrected for an unusual apparent receding velocity component. This velocity comes into play in the computation and provides a noteworthy outcome accountable for the temporal deviation.

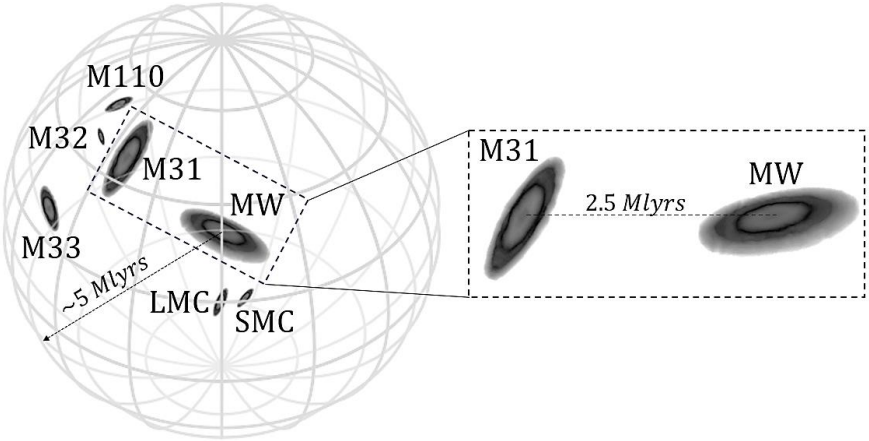

Figure 1. *Schematization of the Local Group embedded in a hypothetical spatial sphere, not to scale, whose radius is about 5 Mlyrs containing the most important galaxies. Andromeda Galaxy (M31) and the Milky Way Galaxy (MW), the latter placed for simplicity in the center, are the two biggest galaxies in the group whose separation is 2.5 Mlyrs based on the most current measurements. Due to these factors, they are also strongly gravitationally bound and this allows us to perform investigations in regard to the future encounter over time. We can also identify the Large Magellanic Cloud (LMC), the Small Magellanic Cloud (SMC) both satellite galaxies of the MW. Satellite galaxies of M31 are instead the Triangulum Galaxy (M33), Le Gentil (M32) and the Edward Young Star (M110). Other distant galaxies are actually in this spatial sphere. However, they do not affect the M31-MW orbital motion due to their distance.*

Besides the first-ever calculation of the orbital free-falling time in a non-expanding approach, another peculiarity of the analytical calculation included in this work consists in the introduction of the initial velocity of M31 as boundary condition for the differential equations. In this way, we can predict in advance the behavior of the two main galaxies of the Local Group based on the physical knowledge of orbital dynamics. As mentioned, in our specific case, we introduce a very important velocity parameter, an apparent recession velocity, related to the photon path travelled which is a game-changer in the analysis. Usually, other investigations involve N-Body problem simulations [7] which leads to a 3-5 billion years collision time. Instead, other inquiries involve simulations for different purposes such as for identifying the type of merging galaxy after the collision event [1]. The possibility that the M31 and MW previously collided is argued in other research [8] or even a previous head-on collision between M31 and M32 more than 200 million years ago [9] might modify the background characteristics of the orbital interaction with the MW. Nonetheless, the most accepted value for the orbital free-falling time between M31 and MW is

4.5 $Gyrs$ [10] in the scientific community as well as in the public opinion and this value is our reference for our analytical computation.

M31-MW Standard Orbital Free-Falling Time

With focus on the pair M31-MW, based on the motion equation in a two-body system in the center-of-frame, the acceleration a according to the orbital dynamics can be written as

$$a = r''(t) = -\frac{GM_{tot}}{r^2(t)}, \tag{1}$$

where G is the gravitational constant and $r(t)$ is the variable distance over time in the line of sight between M31 and MW. Equation (1) expresses Kepler's orbital formulation in Newtonian terms [11, 12]. The total mass of the two galaxies together is given by

$$M_{tot} = M_{M31} + M_{MW} \tag{2}$$

The solution to the differential equation of Equation (1) is the coordinate distance $r(t)$ which varies bouncing from higher to lower values during the encounter and then during the merging process. However, only the time required by the two galaxies to encounter is the searched solution of our orbital problem. We name it orbital free-falling time. Multiplying both members by the first derivative of the radial coordinate respect to time, the differential equation assumes the form

$$r''(t)\, r'(t) = -\frac{GM_{tot}}{r^2(t)} r'(t), \tag{3}$$

and after several mathematical steps contained in Appendix A, it yields

$$\int \frac{dr}{\sqrt{2\left(\frac{GM_{tot}}{r}+k_1\right)}} = \int dt. \tag{4}$$

The integral at the right-hand side of the equation is easily solvable whereas we can solve the left-hand integral by introducing a set of new variables. After multiple steps contained in Appendix B, we reach the following in-between result

$$\frac{\sqrt{2}\,GM_{tot}}{\sqrt{k_1^3}}\frac{1}{2}\left\{\frac{1}{\sqrt{\frac{\frac{GM_{tot}}{r}+k_1}{k_1}}\sqrt{1-\frac{1}{\frac{\frac{GM_{tot}}{r}+k_1}{k_1}}}}\frac{1}{\sqrt{1-\frac{1}{\frac{\frac{GM_{tot}}{r}+k_1}{k_1}}}} - \log\left[\frac{1}{\sqrt{\frac{\frac{GM_{tot}}{r}+k_1}{k_1}}\sqrt{1-\frac{1}{\frac{\frac{GM_{tot}}{r}+k_1}{k_1}}}} + \frac{1}{\sqrt{1-\frac{1}{\frac{\frac{GM_{tot}}{r}+k_1}{k_1}}}}\right]\right\} = t + k_2. \tag{5}$$

Subsequently, we can foil many parameters and factor out other ones in Appendix C until we obtain

$$\frac{r}{k_1}\sqrt{\frac{GM_{tot}}{r}+k_1} - \frac{GM_{tot}}{\sqrt{k_1^3}}\cdot\tanh^{-1}\left[\sqrt{\frac{\frac{GM_{tot}}{r}+k_1}{k_1}}\right] = \sqrt{2}(t+k_2), \tag{6}$$

in which we stepped from a logarithmic formulation toward the inverse hyperbolic tangent function, as the two mathematical functions are complementary. This action is required in order to avoid an indeterminate outcome. The implicit solution of the differential equation can be expressed as the new function encompassing all mentioned parameters so far. We can square both members in order to prevent carrying the complex number $i = \sqrt{-1}$ later with us, once we calculate the limit, as follows

$$\phi(r,t) = \left\{\frac{r}{k_1}\sqrt{\frac{GM_{tot}}{r}+k_1} - \frac{GM_{tot}}{\sqrt{k_1^3}}\cdot\tanh^{-1}\left[\sqrt{\frac{\frac{GM_{tot}}{r}+k_1}{k_1}}\right]\right\}^2 - \left[\sqrt{2}\,(t+k_2)\right]^2 = 0. \tag{7}$$

In fact, the orbital free-falling time assumes a characteristic expression for $r \longrightarrow 0$ calculated in Appendix D as

$$\lim_{r\to 0}\phi(t) = \left[\frac{GM_{tot}}{\sqrt{k_1^3}}\cdot\frac{-i\pi}{2}\right]^2 - 2(T+k_2)^2 = 0. \tag{8}$$

Thus, the orbital free-falling time is given by

$$T_{fall} = \frac{\pi G M_{tot}}{2\sqrt{2k_1^3}} - k_2, \tag{9}$$

which still contains the integration constants k_1 and k_2 to calculate. In order to introduce the velocity boundary condition, we have to derive Equation (7) with respect to time in Appendix E starting from

$$\frac{d\phi(r,t)}{dt} = \frac{d}{dt}\left\{\left\{\frac{1}{k_1}r\sqrt{\frac{GM_{tot}}{r}+k_1} - \frac{GM_{tot}}{\sqrt{k_1^3}}\cdot\tanh^{-1}\left[\sqrt{\frac{\frac{GM_{tot}}{r}+k_1}{k_1}}\right]\right\}^2 - \left[\sqrt{2}\,(t+k_2)\right]^2\right\} = 0, \tag{10}$$

until reaching an expression in which we factor out the first derivative with respect to time of the relative radial position as

$$r'(t) = \frac{2\sqrt{k_1^3}(t+k_2)\sqrt{\frac{GM_{tot}}{r}+k_1}}{r\sqrt{k_1}\sqrt{\frac{GM_{tot}}{r}+k_1}-GM_{tot}\cdot\tanh^{-1}\left[\sqrt{\frac{\frac{GM_{tot}}{r}+k_1}{k_1}}\right]}. \quad (11)$$

The first boundary condition to analyze is the own total relative initial velocity v_0 of M31 associated to the relative blueshift and transversal motion both implicitly corrected for the Sun-Earth-MW motion, or rather

$$r'(0) = v_0 = \frac{2k_2\sqrt{k_1^3}\sqrt{\frac{GM_{tot}}{r}+k_1}}{r\sqrt{k_1}\sqrt{\frac{GM_{tot}}{r}+k_1}-GM_{tot}\cdot\tanh^{-1}\left[\sqrt{\frac{\frac{GM_{tot}}{r}+k_1}{k_1}}\right]}, \quad (12)$$

which allows to us to determine the coefficient k_2 equal to

$$k_2 = \frac{v_0\left\{r\sqrt{k_1}\sqrt{\frac{GM_{tot}}{r}+k_1}-GM_{tot}\cdot\tanh^{-1}\left[\sqrt{\frac{\frac{GM_{tot}}{r}+k_1}{k_1}}\right]\right\}}{2\sqrt{k_1^3}\sqrt{\frac{GM_{tot}}{r}+k_1}}. \quad (13)$$

It is important to stress that in the orbital free-falling time the total velocity v_0 is the sum of the radial and transverse components as we are effectively dealing with an orbital two-body problem. Even if we decided to consider only the radial velocity in a radial free-falling time, this initial velocity would increase up to the galaxy encounter but we do measure only one value for a specific redshift distance. For this reason, the discussion of an orbital free-falling time with one reliable average total velocity v_0 is very complete and it is equivalent to consider a radial free-falling approach with increasing radial velocities over time. In effect, we average the velocity distribution by considering the measured radial velocity at the M31-distance and an average high transverse velocity [5] combined together. Therefore, only with one total velocity v_0, we take into account the impact to the free-falling time provided by increasing velocities up to the encounter process. Given this and plugging the expression of the coefficient k_2 into the solution to the differential equation from Equation (6) for $t = 0$ corresponding to the current observed distance $r = d_{M31}$ of Andromeda Galaxy, we can write from Appendix F that

$$\frac{d_{M31}}{k_1}\left(\sqrt{\frac{GM_{tot}}{d_{M31}}+k_1}-\frac{v_0}{\sqrt{2}}\right) = \frac{GM_{tot}}{\sqrt{k_1^3}}\cdot\tanh^{-1}\left[\sqrt{\frac{\frac{GM_{tot}}{d_{M31}}+k_1}{k_1}}\right]\left(1-\frac{v_0}{\sqrt{2}\sqrt{\frac{GM_{tot}}{d_{M31}}+k_1}}\right). \quad (14)$$

As shown in Appendix G, Equation (14) can be zero in one specific case both from the left-hand and right-hand side of the equation, exactly when

$$k_1 = \frac{v_0^2}{2}-\frac{GM_{tot}}{d_{M31}}. \quad (15)$$

Due to this, we can rewrite the expression of the coefficient k_2 from Equation (13), this time calculated for $r = d_{M31}$, from Appendix H, as

$$k_2 = \frac{v_0 d_{M31}}{2\left(\frac{v_0^2}{2}-\frac{GM_{tot}}{d_{M31}}\right)}-\frac{GM_{tot}}{\sqrt{2\left(\frac{v_0^2}{2}-\frac{GM_{tot}}{d_{M31}}\right)^3}}\cdot\tanh^{-1}\left(\frac{v_0}{\sqrt{2\left(\frac{v_0^2}{2}-\frac{GM_{tot}}{d_{M31}}\right)}}\right). \quad (16)$$

At this point, substituting the expression of the coefficients k_1 from Equation (15) and k_2 from Equation (16) into Equation (9), we can calculate the orbital free-falling time as the sum of three different contributions as follows

$$T_{fall} = \frac{\pi GM_{tot}}{2\sqrt{2\left(\frac{v_0^2}{2}-\frac{GM_{tot}}{d_{M31}}\right)^3}}-\frac{v_0 d_{M31}}{2\left(\frac{v_0^2}{2}-\frac{GM_{tot}}{d_{M31}}\right)}+\frac{GM_{tot}}{\sqrt{2\left(\frac{v_0^2}{2}-\frac{GM_{tot}}{d_{M31}}\right)^3}}\cdot\tanh^{-1}\left(\frac{v_0}{\sqrt{2\left(\frac{v_0^2}{2}-\frac{GM_{tot}}{d_{M31}}\right)}}\right). \quad (17)$$

Furthermore, for an initial velocity equal to zero, or rather $v_0 = 0$, we obtain

$$T_{fall,v_0=0} = \frac{\pi}{2}\sqrt{\frac{d_{M31}^3}{2GM_{tot}}}, \quad (18)$$

which is exactly the free-falling time in the scientific literature under the assumption that M31 has no initial velocity. It is equivalent to omit the radial velocity determined through the blueshift and to calculate the free-falling time under the sole influence of the gravitational interaction. This instance does not represent the reality of the M31-MW system as we effectively measure a blueshift and moreover, any incoming galaxy has effectively an initial velocity in space, unless for some coincidences the pull of another neighbor galaxy behind places it into an equilibrium configuration with no velocity. It is important to underline that we discuss the gravitational interaction in terms of gravitational pull as we analyze a Keplerian/Newtonian framework rather than an Einsteinian one. In the latter, the pull would be described by the deformation of each galactic space-time. Except for some corrections, the two frameworks can be considered interchangeable. Going back to our problem, for calculation purposes and in order to visually improve the formulation of the free-falling time, we can simplify Equation (17) as follows

$$T_{fall} = \frac{\pi GM_{tot}}{2\sqrt{2\xi^3}}-\frac{v_0 d_{M31}}{2\xi}+\frac{GM_{tot}}{\sqrt{2\xi^3}}\cdot\tanh^{-1}\left(\frac{v_0}{\sqrt{2\xi}}\right), \quad (19)$$

where we defined the new parameter ξ expressing the square of a velocity as

$$\xi = \frac{v_0^2}{2} - \frac{GM_{tot}}{d_{M31}}. \quad (20)$$

Since the inverse of the arctangent hyperbolic function can be written, for definition and going back to a previous formulation adopted in the derivation, in logarithmic terms, and in turn expanded according to a Taylor expansion series, the following approximation is also valid

$$\tanh^{-1}\left(\frac{v_0}{\sqrt{2\xi}}\right) \cong \frac{1}{2} log\left(\frac{1+\frac{v_0}{\sqrt{2\xi}}}{1-\frac{v_0}{\sqrt{2\xi}}}\right) \cong \frac{v_0}{\sqrt{2\xi}} + \frac{1}{3}\left(\frac{v_0}{\sqrt{2\xi}}\right)^3 + \frac{1}{5}\left(\frac{v_0}{\sqrt{2\xi}}\right)^5. \quad (21)$$

Due to the approximation of Equation (21), it follows that the orbital free-falling time of Equation (19) becomes

$$T_{fall} = \frac{\pi GM_{tot}}{2\sqrt{2\xi^3}} - \frac{v_0 d_{M31}}{2\xi} + \frac{GM_{tot}}{\sqrt{2\xi^3}}\left[\frac{v_0}{\sqrt{2\xi}} + \frac{1}{3}\left(\frac{v_0}{\sqrt{2\xi}}\right)^3 + \frac{1}{5}\left(\frac{v_0}{\sqrt{2\xi}}\right)^5\right], \quad (22)$$

$$T_{fall} = 1.437 \cdot 10^{17} \text{ sec} = 4.55\ Gyrs. \quad (23)$$

The relevant physical parameters in the formula of Equation (22) and Equation (23) are the following, starting from the gravitational constant

$$G = 6.674 \cdot 10^{-11} \frac{m^3}{Kg\ sec^2}, \quad (24)$$

proceeding with the mass of Andromeda Galaxy [13]

$$M_{M31} = 2.98 \cdot 10^{42}\ Kg, \quad (25)$$

as well as the Milky Way mass [14]

$$M_{MW} = 1.15 \cdot 10^{42}\ Kg, \quad (26)$$

and the total mass mathematically provided in the center-of-mass frame from Equation (2) but now with a numerical value equal to

$$M_{tot} = M_{M31} + M_{MW} = 4.13 \cdot 10^{42}\ Kg, \quad (27)$$

and last but not least, the current distance measured between Andromeda and the Milky Way [14] equal to

$$d_{M31} = 2.365 \cdot 10^{22}\ m = 2.5\ Mlyrs, \quad (28)$$

determined by means of cepheid investigations [15]. As mentioned in the previous paragraphs, the total relative velocity v_0 is regarded as the sum of the radial component [2], which we measure through the blueshift and the related corrections, and the transverse velocity [6] with similar corrections. Once again, v_0 depicts and orbital scenario in this analytical calculation in which, by considering this total velocity seen like an average one, we are actually including the overall velocity increase in the M31-MW encounter. Otherwise, the alternative to this assumption would be a numerical simulation, however, not involved in this investigation. Therefore, the total orbital velocity assumes the following value

$$v_0 = \sqrt{v_r^2 + v_t^2} = \sqrt{-110000^2 + 224499.45^2} = 250000\ \frac{m}{sec} = 250\ \frac{Km}{sec}. \quad (29)$$

Based on the Doppler-analysis (2), the radial velocity of Andromeda intrinsically accounts for the velocity vector component of the MW in the Local Group as well as the velocity component of the Sun in the MW same like the velocity component of Earth in the solar system. These are implicit corrections performed by other inquiries. However, the M31-MW real orbital free-falling time should take into account many more parameters: we neglect the empirical correction factors for the eccentricity between mergers, which is not well known in advance, as well as the influence of the tidal forces due to the pull of the gravitational fields between both galaxies. This is because we can interpret the tidal acceleration as a stripping effect experienced by the colliding galaxies which does not influence the radial position of their center-of-mass. Moreover, another important parameter comes into play: the dynamical friction in the center-of-mass frame. As we calculate, it makes the orbital free-falling time longer but it is a very small value. Under the assumption that the total relative velocity of M31 toward MW remains unchangeable during the free-fall, the extra required free-fall time can be qualitatively expressed by the following formula

$$T_{df} = \frac{v_0}{|a_{df}|} = 1.99 \cdot 10^{14}\ sec \cong 0.01\ Gyrs, \quad (30)$$

where a_{df} is the deceleration associated to the dynamical friction from a simplified form of Chandrasekhar's formulation [16-18] given by

$$a_{df} = -\frac{4\pi G^2 M_{tot}\, \rho_{star,IGM}\, ln(\Lambda)}{v_0^2} = -1.251 \cdot 10^{-9}\ \frac{m}{sec^2}, \quad (31)$$

where, in turn

$$ln(\Lambda) = 5, \quad (32)$$

with Λ a dimensionless parameter (despite of the symbol, it is absolutely not related to dark energy or the cosmological constant) for merging galaxies. Moreover, the density of stars in the intergalactic medium (IGM) associated to the Local Group between M31 and MW [19] is

$$\rho_{star,IGM} \cong 10^{-3}\ \frac{stars}{pc^3} = 3.4 \cdot 10^{-53}\ \frac{stars}{m^3} = 6.76 \cdot 10^{-23}\ \frac{Kg}{m^3}, \quad (33)$$

in the hypothesis that an average star has a Sun-like mass [20] or rather

$$M_s = 1.989 \cdot 10^{30}\ Kg. \quad (34)$$

Equation (33) provides a reliable value as the density of matter between merging galaxies is expected to be slightly higher than the matter density of the Universe as, in the perspective of the M31-MW system in its whole, more matter is diffuse in the galaxy halos and beyond. Therefore,

$$\rho_{star,IGM} = 6.76 \cdot 10^{-23} \frac{Kg}{m^3} > 2.68 \cdot 10^{-27} \frac{Kg}{m^3} = \rho_{Univ}. \quad (35)$$

Ultimately, considering all temporal factors from Equation (23) and Equation (30) together, we can write that

$$T_{fall,real} = T_{fall} + T_{df} = 4.55 + 0.01 = 4.56\, Gyrs. \quad (36)$$

This calculation represents the reality of the two-body problem Andromeda-Milky Way under the assumption that there is no eccentricity in the orbital free-fall of the two galaxies and that other galaxies in the Local Group do not play any role in the falling-orbit as well as in the merging process and therefore, they do not influence the overall orbital falling-time. We include the dynamical friction and its contribution is very small. Furtherly, we can also neglect the current position of M31 at the time, today, when we detect the photons. In this span of time photons of light travelled towards us on a straight path in a time equal to

$$t_{trav} = \frac{d_{M31}}{c} = 7.889 \cdot 10^{13} sec \cong 0.003\, Gyrs, \quad (37)$$

which is practically negligible with respect to the order of magnitude of the orbital free-falling time. Accordingly, the distance travelled by M31 during this period of time is also negligible as in the order of $10^{19}\, m \cong 10^{-3}\, Mlyrs$. For this reason, we omit these values in the calculation. Thus, the result of Equation (36) remains unaffected.

2. Non-expanding Universe Framework

Although the standard model parametrized by means of the Lambda Cold Dark Matter (ΛCDM) cosmology is well established in the scientific community since almost a century, observational data diverge permanently from the theory and from the expectations of the research departments which are stuck in their mindset. We can relate these facts and argumentations in a huge checklist starting, from instance, from the implicit assumption that the gravitational bound of the galaxies in any cluster dominates over the expansion of space. Whilst it is stated that Local Group is decoupled from the space expansion [1], the photon energy loss in a non-expanding framework is strongly coupled instead. Cosmologists infer a space expansion but yet they can observe intact cluster of galaxies not ripped apart by the stretching of space inducing them to make statements on the cohesion of the galaxies in any cluster. From a theoretical standpoint, it might also mean absence of space expansion. However, in a tired light process, we have to account for the apparent recession velocities of the photons of light associated to the redshift of the observed galaxy. It is for the first time ever included in the core of an investigation like this. We show this concept in Figure 2. Moreover, we will approach again the subject in Section 2.2 in much greater detail.

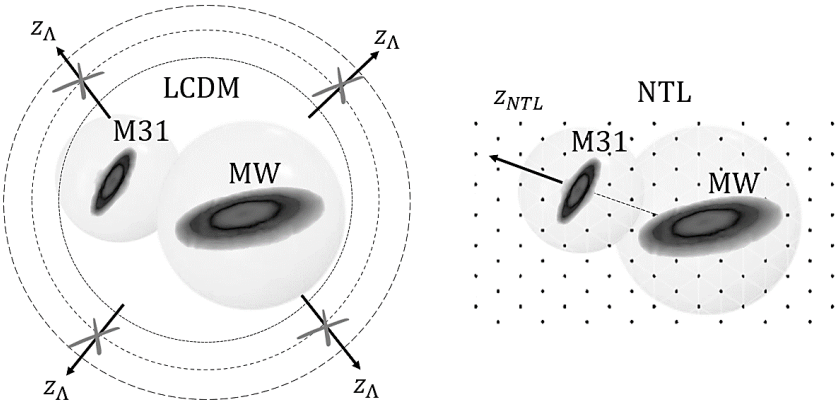

Figure 2. *Difference between the conceptual representation of the Andromeda (M31) - Milky Way (MW) system based on the standard expanding space model (ΛCDM) on the left and a non-expanding tired light-dominated model (NTL) on the right. In the first scenario, the gravitational interaction between the two galaxies, represented by potential gravitational spheres in the background, dominates over the expansion of space or rather over its dark energy redshift value* z_Λ *as result from Friedmann equations in GR. What lies in space between the galaxies and how it might influence the photons, is not conceived in standard cosmology except for the existing component in the stress-momentum tensor in GR. In the second scenario, the redshift results exclusively from the photon energy loss in space after multiple interactions with free crystallized electrons in space. In this case the medium plays an important role in the calculation. This provides a redshift* z_{NTL} *corresponding to an apparent recession velocity in Doppler-shift terms not only for the M31-MW pair but also for any system emitter-observer. Accordingly, this aspect affects the relative motion between the two galaxies as well as the orbital free-falling time. In our figure, the relative motion is implicitly considered as the main purpose is to show the extra velocity, or redshift, involved in the non-expanding framework as well as the missing expansion contribution in the standard model.*

For instance, there are also some inconsistencies for one of the pillars of the standard model such as the dark matter. Objectively, the latter starts to suffer the lack of evidence which leads therefore to the search for alternative solutions not only on cosmological scale [21] but also on local one [22]. We can also mention the vague definition of dark energy driving the alleged expansion of space. It comes out in a pure mathematical way from Einstein's General Relativity (GR) by imposing the space expansion as boundary conditions prior to understanding its effect. It comes from Friedmann's equations and it is claimed to be strictly related to the redshift in the absorption lines of the galactic spectra, already starting from Hubble's very first observational work. Basically, they impose the space expansion due to the redshift measurement explanation of the galactic spectra. This inevitably leads the mathematics toward an expanding space solution. Absurdly, in a hypothetical different scenario, if we assumed a redshift exclusively due to a time dilation in GR, as other scientists do, we would obtain a redshift within this physical meaning as output. Other scientists impose, for instance, a variable speed of light rather than an expanding space. As one can notice, there are different valid scenarios in cosmology. In practice, the cosmological redshift can be differently interpretated and despite of that, the GR framework can remain valid as in the case of a tired light-dominated Universe [23]. A good way to work consists in founding different departments, each working on a theory, in order to exchange scientific information in order to debunk or confirm one model over the other. This is something that does not regularly happen in the astrophysics/cosmology policy or working culture. Unexpectedly, alternative frameworks based on known physics take quietly hold and give an explanation to many phenomena in astrophysics and cosmology nowadays. Lastly, another cosmological pillar, the age of the Universe, $13.8\,Gyrs$ thus far, is nowadays debated if not even doubled in time in order to fit the observational data of the James Webb Space Telescope (JWST) [24]. This fact literally disrupts all recognized cosmological equations and their physical meaning. This high-technologic instrument of the mankind in the extended infrared-field provides new unexpected insights [25, 26] concerning the evolutionary stage of the galaxies through their spectra. Many galaxies are found in an evolutionary stage incompatible with the age of the Universe. All these matters offer to us a green-light in the alternative research and mindset in astrophysics and cosmology. For this reason, we focus on the influence that the apparent velocity component associated to a tired light redshift has on the M31-MW orbital free-falling time.

2.1. Photon Transit in the IGM and Photon Energy Loss

Our focus is on the Tired Light (TL) theory and specifically on the recent development given by multiple interactions between photons of light with crystallized electrons in the intergalactic medium conceived by Ashmore's New Tired Light (NTL) [27]. In the past, Nernst [28] was the first scientist to postulate a Tired Light (TL) process even before Zwicky's physics [29]. Contrary to appearances, Zwicky does not explicitly introduce the current tired tight idea as we mean it nowadays with Ashmore's NTL arguments or with other different TL approaches rarely found in the scientific literature. Indeed, Zwicky postulated that photons of light travelling through a mass distribution in space, consisting in space particles, lose momentum assuming that the gravitational interaction is not transmitted instantaneously but rather with the speed of light according to the theory of the retarded potentials. This led to a redshift direct proportional to the distance travelled and also function of a new-defined perturbation distance related to this mass distribution. In some respects, he pointed out the possibility the photons lose energy in space but only afterwards other prominent scientists in the antagonist (to the ΛCDM) scene imposed the exponential TL formula and provided arguments in favor [30] and against [31] this physics approach. Recently, first valuable attempts to derive the exponential redshift TL formula with the distance travel by the photons has been conducted by Laviolette [32] until Ashmore [27] who provided the first concrete and tangible explanation to what TL redshift is. Ashmore is the first ever scientist to derive the TL exponential formula, Equation [38] in next section, in a detailed manner also introducing a feasible redshift mechanism: photons lose energy being absorbed and re-emitted by crystallized electrons in the IGM as shown in Figure 3. The electrons recoil at each photon transit and perform a Simple Harmonic Motion (SHM) as described in Quantum Electrodynamics. Moreover, the Hubble constant has a characteristic value function of the electron properties included the number electron density in the medium in a very innovative and observational-based manner.

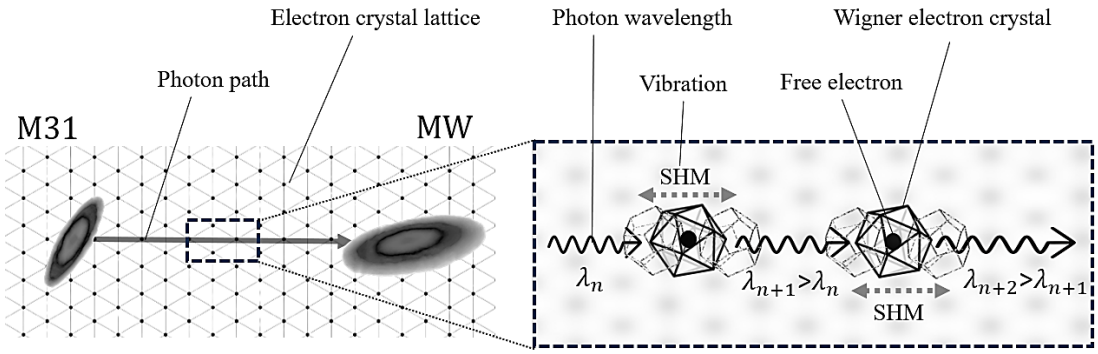

Figure 1. *Schematization of the NTL redshift mechanism. Photons of light travel in the IGM through an electron crystal lattice medium which absorb and re-emit photons in a multiple interaction process photons-electrons from the emitter to the observer. The electron crystal lattice composes a transparent grid in space through which photons travel on a straight line rather than exhibiting a scattering process. For this reason, we do not detect any blurred image. At each electron-transit the photons spend a tiny amount of energy given for the recoil of the electron itself which vibrates performing a simple harmonic motion according to Quantum electrodynamics. Accordingly, the photons are redshifted after each electron transit up to the observer, or rather their wavelengths are longer than the initial ones* $\lambda_N > \lambda_{N-1} > \cdots > \lambda_1$ *if we hypothetically assume N total interaction events, where in between we observe n, n+1, n+2 events and so on, from emitter to observer.*

Due to the electron crystallization predicted by Wigner last century [33, 34] electrons arrange themselves on a crystal lattice in the IGM under specific conditions. Intuitively and based on the physics, electrons crystallize at cryogenic temperature in the IGM. However, Solid-state physics allows the crystallization not only at temperatures close to the absolute zero but also at different temperatures as long as a specific condition is verified: the Coulomb potential energy of the electron has to overcome its kinetic energy by a factor 175 in order to crystallize [35, 36]. A comprehensive mathematical overview of the NTL theory, which also includes the previous condition, is contained in Appendix I. This non-expanding framework has been confirmed in many astrophysical research fields, and it is currently in progress. Published papers embrace the Fast Radio Bursts (FRB's) [37, 38] up to the center-to-limb problem [39] in the solar corona, passing by the anomaly the Pioneer space probes [40], the explanation of the Cosmic Microwave Background Radiation [41], and last but not least the explanation of cosmological redshift and the Hubble tension according to Trinchera's Transit Physics [23] which relies on the redshift-independent extragalactic distances (NED-D) and involves a specific GR solution. In this inquiry, we demonstrate that the M31-MW orbital free-falling time is dictated from this tired light approach as well.

2.2. M31-MW Orbital Free Falling-time Based on Photon Energy Loss

In an expanding Universe, the space expansion is thought to be negligible in local environments such as in the Local Group. Both the Milky Way Galaxy and Andromeda Galaxy belong to the Local Group and therefore their gravitational interaction dominates over the expanding Universe. The forces between galaxies due to the gravitational binding supersede the stretch of space. For this reason, no cosmological calculation based on the ΛCDM model appears in the equation of the free-falling time, neither in the standard cosmology literature nor in this section of the investigation: it is irrelevant and uninfluential to this local scale problem. It is the reason why the blueshift of Andromeda is only dictated by the relative approach velocity of M31 toward the MW. From the blueshift, interpretated through the Doppler shift, we infer the motion of one galaxy respect to the other, once again, as long as corrections for the combined Earth-Sun-MW motion are implicitly considered. However, if we switch mindset and consider a non-expanding approach, the framework is slightly different and it causes a different result in terms of orbital free-falling time.

Considering a TL approach and specifically the NTL mindset, even at local distances photons lose energy through space as they interact with free crystallized electrons forming such as an oscillating grid or lattice in space. The photon energy loss, and the way the crystallized electrons are arranged in space, supplies the energy necessary for the vibration of the lattice. This causes the photons to lose energy and to exhibit a redshift or namely a longer wavelength at each electron crystal transit. In Doppler-shift terms, it is equivalent to apparent recession velocities. Distances between galaxies or any astronomical object are well established in space (if we have a reliable measurement method such as Cepheids for M31) and these objects interact gravitationally with each other. The apparent recession velocity, whose redshift increases exponentially with the distance, is an integral part of our calculation: it provides the illusion of a receding galaxy, M31 in our investigation field. A steady point is that there is no expansion of space involved in our argument but only the illusion of a receding motion due to the photon energy loss in space. Clearly, the apparent recession velocity associated to a photon energy loss is physically not related to the proper motion of the observed galaxy. However, despite we identify two different processes, their velocity contributions cross over each other. Precisely due to these reasonings, if we measure a

blueshift for Andromeda Galaxy, the relative amount of velocity toward the Milky Way Galaxy is in the reality much higher than expected as the M31 velocity component has to overcome its own apparent recession velocity in the other direction associated to the photon energy loss in space. This concept is visually shown in the velocity vector illustration of Figure 4 as well as in the schematization of Figure 5.

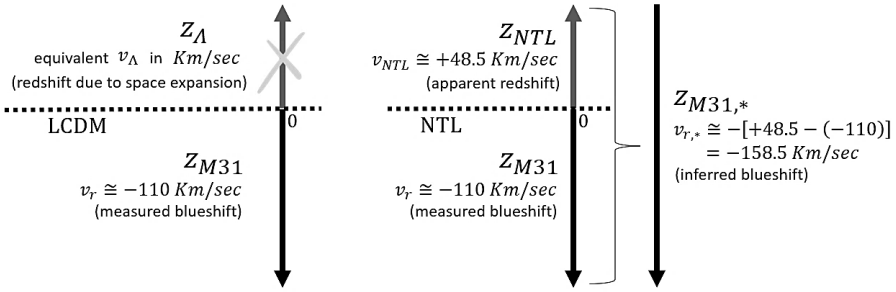

Figure 4. *On the right, the inferred relative radial velocity between Andromeda (M31) and Milky Way (MW) due to the velocity contribution given by the apparent recession velocity associated to a tired light process or rather by a photon energy loss. In order to reach an approach velocity equal to -110 Km/sec, the real approach velocity of Andromeda Galaxy (M31) has to be much bigger. The latter has to overcome the NTL receding velocity vector until reaching -158.5 Km/sec. On the left, we can see the known relative radial velocity of Andromeda. The space expansion, which would cause the separation of the two galaxies or at least a tiny opposing velocity/force, is completely neglected from the standard model perspective, as the forces associated to the gravitational interaction, in Newtonian terms, overcome those associated to the space expansion. For this reason, the approach velocity remains as it is according to the ΛCDM mindset but not based on a NTL one.*

According to the NTL process, by knowing the distance between Andromeda and the Milky Way from Equation (28), we can calculate the redshift as

$$z_{NTL} = e^{\frac{H_{NTL} d_{M31}}{c}} - 1 = 1.617 \cdot 10^{-4}, \tag{38}$$

in which the Hubble constant expressing now a photon energy loss in space is given by

$$H_{NTL} = \frac{2hr_e n_e}{m_e} = 2.05 \cdot 10^{-18}\ \frac{1}{sec} = 63.26 \frac{Km}{\sec Mpc}, \tag{39}$$

meticulously derived in Ashmore's published papers whereas the speed of light is

$$c = 299792458\ \frac{m}{sec}. \tag{40}$$

It is worth to stress that the NTL Hubble constant is quite smaller than the estimate Hubble constant in standard cosmology also in the so-called Hubble tension problem:

$$H_{NTL} = 63.26 \frac{Km}{\sec Mpc} < 67 \div 74 \frac{Km}{\sec Mpc} = H_{LCDM}. \tag{41}$$

From the perspective of a NTL researcher, Equation (41) has an obvious physical meaning as cosmologists are still mistakenly interpreting the Hubble constant as an expanding ratio of the Universe whereas it is precisely the photon energy loss parameter for us or also a synonym of apparent recession velocity of any astronomical object. It is well known that the classic Hubble constant varies depending on the region of space and on the measurement method undertaken. Instead, our Hubble constant strictly depends from the electron properties through which photons interact in space. Accordingly, the Hubble tension characterizes a photon energy loss with increasing number electron densities depending on the astronomical object under consideration [23]. Each astronomical object has its own environment and number electron density distributions: it is valid between Earth and the Sun, in Quasar regions and also between galaxies where we measure the smallest astrophysical number electron density equal to $n_e = 0.5\ el/m^3$ [38]. This reasoning might imply that Quasars are closer in space than expected. Going back to our M31-MW problem, according to the Hubble approximation valid for small scales or non-cosmological distances, and based on a reasoning in Doppler-shift terms, the equivalent apparent recession velocity of M31 is accordingly given by

$$v_{NTL} = c\, z_{NTL} = 48484.9 \frac{m}{sec} \cong 48.5\ \frac{km}{sec}. \tag{42}$$

Due to these considerations, we can calculate the real effective relative radial velocity between Andromeda and the Milky Way as

$$v_{r,*} = -(v_{NTL} - v_r) = -[+45.8 - (-110)] = -158484.9\ \frac{m}{sec} \cong -158.5\ \frac{km}{sec}, \tag{43}$$

where the approach velocity is mathematically represented by the negative sign, imposed in the formulation.

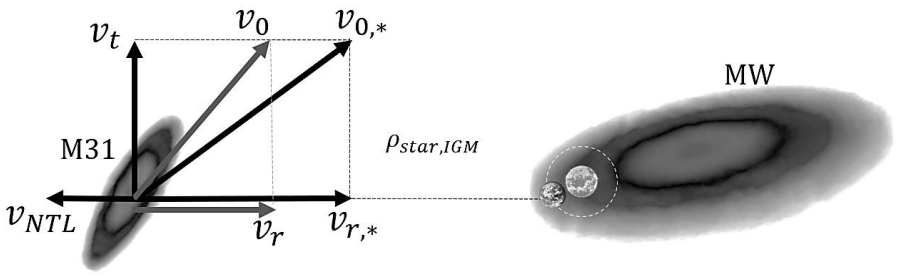

Figure 5. *Schematization of M31-MW system, included Earth and the Sun, not to scale. We can observe the difference between the total relative velocity M31-MW, given by the sum (v_0) of the transverse (v_t) and the radial velocity (v_r) in the current understanding of the M31 radial blueshift, and the total relative velocity ($v_{0,*}$), given by the sum of the same transverse velocity (v_t) and the radial velocity ($v_{r,*}$) that includes this time the apparent recession velocity (v_{NTL}) due to photon energy loss in space in a tired light (NTL) process. The latter triggers a bigger blueshift value than estimated in the scientific literature. All velocities are intrinsically corrected for the MW-Sun-Earth motion components.*

Once again, it is very important to point out how the real radial velocity is much higher than the estimated one from standard cosmology as the photon energy loss provides another important component, therefore,

$$|v_{r,*}| = 158.5 \frac{km}{sec} > 110 \frac{km}{sec} = |v_r|. \quad (44)$$

Keeping the estimated transverse velocity of M31 unchanged, the sum of the components gives out a new value for the inferred total velocity component as follows

$$v_{0,*} = \sqrt{v_{r,*}^2 + v_t^2} = \sqrt{-158484.9^{\,2} + 224499.45^2} = 274804.4 \frac{m}{sec} \cong 274.8 \frac{km}{sec}. \quad (45)$$

In the light of this new approach, the parameter previously expressed by Equation (20) becomes now

$$\xi_* = \frac{v_{0,*}^2}{2} - \frac{GM_{tot}}{d_{M31}}, \quad (46)$$

leading toward a new orbital free-falling time from Equation (22) as

$$T_{fall,*} = \frac{\pi GM_{tot}}{2\sqrt{2\xi_*^3}} - \frac{v_{0,*}\, d_{M31}}{2\xi_*} + \frac{GM_{tot}}{\sqrt{2\xi_*^3}}\left[\frac{v_{0,*}}{\sqrt{2\xi_*}} + \frac{1}{3}\left(\frac{v_{0,*}}{\sqrt{2\xi_*}}\right)^3 + \frac{1}{5}\left(\frac{v_{0,*}}{\sqrt{2\xi_*}}\right)^5\right], \quad (47)$$

$$T_{fall,*} = 5.372 \cdot 10^{16}\,\text{sec} = 1.70\ Gyrs. \quad (48)$$

It also implies that the dynamic friction deceleration of Equation (31) becomes now

$$a_{df,*} = -\frac{4\pi G^2 M_{tot}\, \rho_{star,IGM}\, ln(\Lambda)}{v_{0,*}^2} = -1.035 \cdot 10^{-9} \frac{m}{sec^2}, \quad (49)$$

and consequently, the delay respect to the theoretical value of the orbital free-falling time is

$$T_{df,*} = \frac{v_{0,*}}{|a_{df,*}|} = 2.652 \cdot 10^{14}\ sec \cong 0.01\ Gyrs, \quad (50)$$

with no relevant deviation compared to the previous value of Equation (30). Summing up the two main effects, the theoretical time value from Equation (48) and that one due to the resistance in space from Equation (50), the real or effective total free-falling time assumes the following value

$$T_{fall,real,*} = T_{fall,*} + T_{df,*} = 1.70 + 0.01 = 1.71\ Gyrs. \quad (51)$$

Based on this, it is very clear that the comparison between the same parameter in two different approaches, expanding space from Equation (36) and non-expanding-space from Equation (51), allow us to corroborate that there is an important temporal deviation:

$$T_{fall,real,*} = 1.71\ Gyrs \ll 4.56\ Gyrs = T_{fall,real}. \quad (52)$$

The result of Equation (51) indicates that the real effective orbital free-falling time is smaller when we consider that the approach velocity of Andromeda is much faster than expected. This statement is based on the physics of a non-expanding framework applied to the falling orbit of the two-body M31-MW system. In Figure 6, we can visually observe the steps that lead to the two galaxies to encounter and then merge together with their characteristic orbital free-falling time.

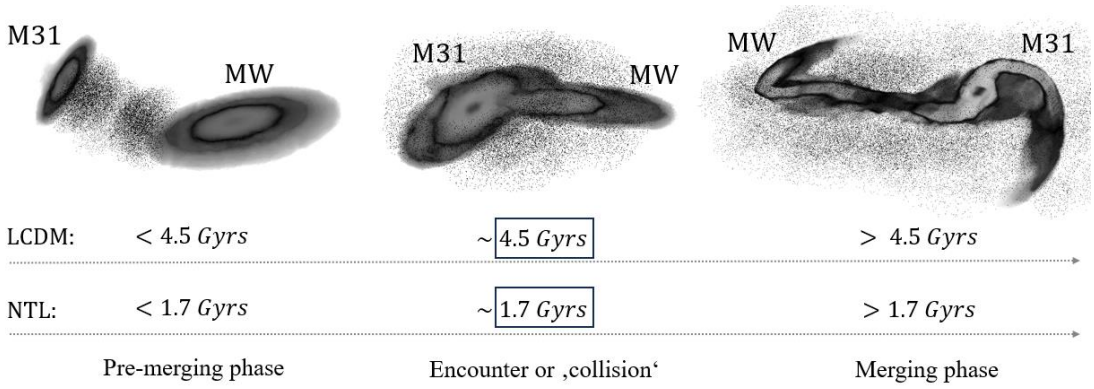

Figure 6. *Physical and Temporal schematization of the encounter process between Andromeda Galaxy (M31) and the Milky Way (MW) from the point of view, on one side, of the standard model (ΛCDM) characterized only by a gravitational interaction as the space expansion is negligible and, on the other side, of non-expanding tired light-dominated Universe (NTL) which, besides the gravitational interaction, conceives an apparent recession velocity which modifies the M31-MW relative velocities. The galaxies gravitationally attract themselves causing the strip of the outer gas and stellar regions. At the orbital free-falling time the galaxies encounter even if it is a go-through process without a clash: 4.5 Gyrs for the standard model against 1.7 Gyrs for a non-expanding Universe. Both galaxies gravitationally switch side while they are stripped apart keeping a characteristic elongated shape observed many times in real merging events in the Universe by telescopes. This kind of observational images are like frozen frames in time which provide information about the orbital dynamics also confirmed by numerical simulations. Eventually, the galaxies will merge into one-single galaxy due to the strong gravitational pull.*

In order to measure an approach velocity of $v_r = -110\ Km/sec$, it means that the main velocity vector has to be greater than this value in order to compensate the effect of the apparent recession velocity due to a tired light process or rather the energy loss of photons through space, as represented in previous Figure 4 and Figure 5. Moreover, we can assign a specific order of magnitude to this temporal deviation by calculating the orbital falling-time ratio between M31-MW as follows

$$R_T = \frac{T_{fall,real}}{T_{fall,real,*}} = \frac{4.56}{1.71} = 2.7, \tag{53}$$

or namely, in a non-expanding and NTL-dominated Universe Andromeda Galaxy will reach the Milky Way Galaxy almost three times faster in time than within an expanding space framework.

3. Discussion and Conclusions

In the context of this scientific investigation characterized by a two-body problem involving the galaxies Andromeda (M31) and the Milky Way (MW), we can objectively draw the following conclusions:

1) as preliminary information in the orbital equations, we calculate the orbital free-falling time in both frameworks considering an initial velocity equal to the total relative velocity between M31 and the MW. This velocity is the sum of the relative radial velocity M31-MW, which accounts for all corrections of the MW motion in the Local Group as well as the motion of the Earth/Sun system in the MW, together with the estimated M31 transverse velocity which accounts for the same corrections. All single velocity values refer to existing published papers: these velocities are, respectively, $v_r = -110\ Km/sec$ (in approach toward the MW) and $v_t = 224.5\ Km/sec$ conformal to the upper-limit for the transverse velocity value according to another specific inquiry from the scientific literature;
2) in the final analysis, the core of this work involves the analytical computation of the difference between the orbital free-falling time based, on one hand, on the standard scientific literature in an expanding Universe framework, equal to $T_{fall,real} = 4.56\ Gyrs$ and close to the value of the scientific literature $T_{fall,astroph.} = 4.5\ Gyrs$ and, on the other hand, on a non-expanding tired light-dominated Universe which results in $T_{fall,real,*} = 1.71\ Gyrs$. In the specific, we adopt the most current NTL physics which can be considered the up-to-date development of the generic TL theory in many respects. In essence, the galaxy encounter between M31 and the MW, improperly mentioned as galactic collision, will occur much earlier than predicted. Eventually, the orbital free-falling time in a non-expanding Universe, intended as the time in the center-of-mass frame from M31 to encounter with the MW, is almost three times (exactly 2.7 times) shorter than the value in an expanding Universe;
3) the difference lies in the impact that the apparent recession velocities associated to the NTL redshift due to the photon energy loss has on the orbital free-falling time in a non-expanding Universe. On the other hand, the unjustified omission of any photon-particle involvement in the current standard model of cosmology does also affect the inconsistency of its outcome and predictions. In short, the discrepancy

between the two approaches lies in the interpretation of the M31 blueshift (or rather the relative velocity M31-MW). The standard model assumes that the expansion of space does not influence the gravitational bound of galaxies in any cluster of galaxies such as in our Local Group therefore, leaving the blueshift value unchanged. In case of a non-expanding tired light-dominated Universe, precisely within the NTL framework, at any distance cosmological or not and specifically in the M31-MW distance, photons of light experience a loss of energy after multiple interactions with crystallized electrons in the IGM. Not by chance, at this distance, we calculate an apparent receding velocity $v_{NTL} = +48.5\, Km/sec$ associated to a NTL mechanism. Photons are absorbed and re-emitted by crystallized Wigner electrons in the IGM on a straight line avoiding the blurring of the images at the receiver. In this process, a specific amount of energy is transferred to the crystallized electron lattice which oscillates according to a simple harmonic motion conceived in the Quantum electrodynamics;

4) with respect to the velocities, all considerations here discussed imply that, in order to measure that blueshift and reach, in turn, a M31-MW relative radial velocity $v_r = -110\, Km/sec$, the module of the velocity vector sum has to include the apparent recession velocity $v_{NTL} = +48.5\, Km/sec$ as this physical value actually works out against the relative motion of the two galaxies. This is exactly the amount to overcome in Doppler-shift terms. Due to this, the effective relative radial velocity assumes the value $v_{r,*} = -158.5\, Km/sec$. This modifies the total relative velocity to a bigger value and accordingly it affects the orbital free-falling time reducing it from $T_{fall,real} = 4.56\, Gyrs$ based on the standard model to $T_{fall,real,*} = 1.71\, Gyrs$ in a non-expanding Universe under the same gravitational boundary conditions. We can stress that based on the solution of the differential equation, there is a strict dependence between the M31-MW orbital free-falling time and the total relative velocity vector parameter as the higher the velocity, the earlier the two galaxies will collide. On the contrary, the time delay due to the dynamic friction forces is directly proportional to v_0^3 in an expanding Universe, or $v_{0,*}^3$ in a non-expanding framework, therefore, increasing for increasing velocities. However, it has a small impact on the total orbital free-falling time due to the tiny amount of matter $\rho_{star,IGM} = 6.76 \cdot 10^{-23}\ Kg/m^3$ between the two galaxies. The latter is insufficient to decelerate the two galaxies in motion but sufficient, specifically due to the number electron density $n_e = 0.5\ el/m^3 = 4.55 \cdot 10^{-31}\ Kg/m^3$ in the IGM, to produce a redshift and, in turn, an apparent recession velocity. In brief, there are enough free electrons in the M31-MW spatial separation to determine a redshift or rather an apparent recession velocity. On cosmological scale, the redshift increases exponentially with the distance whereas on small scales, like our specific case, it can be approximated to a linear relation;

5) besides the gravitational interaction in the orbital dynamics, the physical boundary conditions of the two-body problem include the time delay due to the dynamic friction forces/deceleration in space but not the eccentricity M31-MW, here excluded as it is generally imposed in the scientific literature and not known beforehand, and neither the tidal forces. These forces may only be thought as responsible for the tidal strip of the galaxies during the free-fall process without any influence to both center-of-mass positions in the calculation. Moreover, as there are no numerical simulations performed in this inquiry, we exclude *de facto* the influence that other galaxies of the Local Group (such as the satellite galaxy M33) may have on the main two galaxies. Moreover, it is possible to find out through simple calculations that the position of M31 at the time when we detect the photons, our current day, can also be neglected as the order of magnitude of the distance already covered by M31 is effectively too small to produce significant change to the orbital free-falling time.

A proposal of a follow-up for this inquiry is a numerical simulation considering also the gravitational influence of other galaxies in the Local Group. The fundamental pillar in the parametrization remains the correction of the relative velocities with respect to the Milky Way for the photon energy loss in order to determine a real velocity value as for the NTL process. The relative velocities can be both blueshift or redshift for other galaxies of the Local Group with respect to our perspective in the MW. For instance, assuming that a galaxy exhibits a redshift instead of a blueshift, or rather this galaxy of the Local Group is heading away from the MW due to its proper motion, in this case the apparent receding velocity due to a Tired Light process, in line of sight toward the MW, has to be subtracted from this mentioned value as follows $v_{r,*} = v_r - v_{NTL}$. Instead, in our specific case M31-MW, we summed up the velocities $v_{r,*} = -(v_{NTL} - v_r)$ as we have a relative blueshift measured. The minus sign is imposed as approach velocities have a negative value for definition. The combination of all spatial relative velocities in a N-body problem will provide a specific outcome in the range of values provided by this work. In the meanwhile, the outcome of this inquiry, in the perspective of an alternative physical framework to the expanding space model, is objectively very clear, uncontroversial and lays the foundations for brand new type of research in astrophysics and cosmology not in line with the fruitless fund-based mainstream research.

Abbreviations

M31	Messier 31 or Andromeda Galaxy

MW	Milky Way Galaxy
LMC	Large Magellanic Cloud
SMC	Small Magellanic Cloud
IGM	intergalactic medium
ΛCDM	Lambda Cold Dark Matter
TL	Tired Light
GR	General Relativity

Author Contributions

Alessandro Trinchera is the sole author. The author read and approved the final manuscript.

Funding

This research received no financial support from any funding institution in the public, commercial, or not-for-profit sectors to assist with the preparation of this manuscript, for conducting this study and for covering the article processing charge.

Data Availability Statement

The original contribution presented in the study in terms of the available dataset generated during the investigation can be requested to the corresponding author at any time.

Conflicts of Interest

The author declares no conflicts of interest.

Appendix

Appendix A

$$r''(t)\,r'(t) = -\frac{GM_{tot}}{r^2(t)}r'(t), \tag{A-1}$$

$$\frac{d}{dt}\left\{\frac{1}{2}[r'(t)]^2\right\} = -\frac{GM_{tot}}{r^2(t)}r'(t), \tag{A-2}$$

$$\frac{1}{2}[r'(t)]^2 = \int -\frac{GM_{tot}}{r^2(t)}r'(t)dt, \tag{A-3}$$

$$\frac{1}{2}[r'(t)]^2 = \int -\frac{GM_{tot}}{r^2(t)}\frac{dr}{dt}dt, \tag{A-4}$$

$$\frac{1}{2}[r'(t)]^2 = -GM_{tot}\int \frac{dr}{r^2(t)}, \tag{A-5}$$

$$\frac{1}{2}[r'(t)]^2 = -GM_{tot}\left[-\frac{1}{r(t)}\right] + k_1, \tag{A-6}$$

$$\frac{1}{2}[r'(t)]^2 = \frac{GM_{tot}}{r(t)} + k_1, \tag{A-7}$$

$$\frac{dr}{dt} = \sqrt{2\left(\frac{GM_{tot}}{r} + k_1\right)}, \tag{A-8}$$

$$\int \frac{dr}{\sqrt{2\left(\frac{GM_{tot}}{r}+k_1\right)}} = \int dt. \tag{A-9}$$

Appendix B

$$u = \frac{1}{r}, \tag{B-1}$$

so that

$$du = -\frac{dr}{r^2} == -u^2 dr, \tag{B-2}$$

leading to

$$-\int \frac{du}{u^2\sqrt{2(GM_{tot}u+k_1)}} = t + k_2. \tag{B-3}$$

We can now substitute

$$s = 2(GM_{tot}u + k_1), \tag{B-4}$$

so that

$$ds = 2GM_{tot}du. \tag{B-5}$$

It yields,

$$-\int \left(\frac{GM_{tot}}{\frac{s}{2}-k_1}\right)^2 \frac{1}{\sqrt{s}}\frac{ds}{2GM_{tot}} = t + k_2, \tag{B-6}$$

$$-2GM_{tot}\int \frac{ds}{\sqrt{s}\,(s-2k_1)^2} = t + k_2. \tag{B-7}$$

Furtherly, substituting

$$p = \sqrt{s}, \tag{B-8}$$

so that

$$dp = \frac{ds}{2\sqrt{s}} = \frac{ds}{2p}, \tag{B-9}$$

we obtain

$$-2GM_{tot}\int \frac{2pdp}{p\,(p^2-2k_1)^2} = t + k_2, \tag{B-10}$$

$$-4GM_{tot}\int \frac{dp}{(p^2-2k_1)^2} = t + k_2. \tag{B-11}$$

Focusing on the integrand, we can identify the arctangent form by substituting the new variable

$$p = \sqrt{2k_1}\sec(\vartheta), \tag{B-12}$$

so that

$$dp = \sqrt{2k_1}\sec(\vartheta)\tan(\vartheta)\ d\vartheta. \quad \text{(B-13)}$$

Therefore, the integral becomes

$$-4GM_{tot}\int \frac{\sqrt{2k_1}\sec(\vartheta)\tan(\vartheta)\,d\vartheta}{(2k_1\sec^2(\vartheta)-2k_1)^2} = t + k_2, \quad \text{(B-14)}$$

$$-4GM_{tot}\int \frac{\sqrt{2k_1}\sec(\vartheta)\tan(\vartheta)\,d\vartheta}{4k_1^2[\sec^2(\vartheta)-1]^2} = t + k_2. \quad \text{(B-15)}$$

Since $\tan^2(\vartheta) + 1 = \sec^2(\vartheta)$, we can write that

$$-4GM_{tot}\int \frac{\sqrt{2k_1}\sec(\vartheta)\tan(\vartheta)\,d\vartheta}{4k_1^2\ \tan^4(\vartheta)} = t + k_2. \quad \text{(B-16)}$$

Due to the relations between the trigonometric functions, we can simplify the terms of the integrand as follows

$$\frac{\sec(\vartheta)\tan(\vartheta)}{\tan^4(\vartheta)} = \cot^2(\vartheta)\frac{\sec(\vartheta)\tan(\vartheta)}{\tan^2(\vartheta)} = \cot^2(\vartheta)\frac{1}{\cos(\vartheta)\tan(\vartheta)} = \cot^2(\vartheta)\frac{\cos(\vartheta)}{\cos(\vartheta)\sin(\vartheta)} = \cot^2(\vartheta)\csc(\vartheta) = [\csc^2(\vartheta) - 1]\csc(\vartheta) = \csc^3(\vartheta) - \csc(\vartheta). \quad \text{(B-17)}$$

Therefore,

$$-\frac{\sqrt{2}\,GM_{tot}}{\sqrt{k_1^3}}\int[\csc^3(\vartheta) - \csc(\vartheta)]\,d\vartheta = t + k_2, \quad \text{(B-18)}$$

$$-\frac{\sqrt{2}\,GM_{tot}}{\sqrt{k_1^3}}\{\int \csc^3(\vartheta)\,d\vartheta - \int \csc(\vartheta)\ d\vartheta\} = t + k_2. \quad \text{(B-19)}$$

We can solve each term also introducing a reduction expression such as for the first integral

$$-\frac{\sqrt{2}\,GM_{tot}}{\sqrt{k_1^3}}\left\{\left[-\frac{\cos(\vartheta)\csc^{3-1}(\vartheta)}{3-1} + \frac{3-2}{3-1}\int \csc^{-2+3}(\vartheta)\,d\vartheta\right] - \int \csc(\vartheta)\ d\vartheta\right\}, = t + k_2 \quad \text{(B-20)}$$

and by multiplying and dividing trigonometric functions in the case of the second integral

$$-\frac{\sqrt{2}\,GM_{tot}}{\sqrt{k_1^3}}\left\{-\frac{\cos(\vartheta)\csc^2(\vartheta)}{2} + \frac{1}{2}\int \csc(\vartheta)\,d\vartheta - \int \csc(\vartheta)\ d\vartheta\right\} = t + k_2. \quad \text{(B-21)}$$

Once again due to trigonometric functions we can write that

$$\cos(\vartheta)\csc^2(\vartheta) = \cos(\vartheta)\frac{1}{\sin^2(\vartheta)} = \frac{\cos(\vartheta)}{\sin(\vartheta)}\frac{1}{\sin(\vartheta)} = \cot(\vartheta)\csc(\vartheta). \quad \text{(B-22)}$$

Therefore,

$$-\frac{\sqrt{2}\,GM_{tot}}{\sqrt{k_1^3}}\left\{-\frac{1}{2}\cot(\vartheta)\csc(\vartheta) - \frac{1}{2}\int \csc(\vartheta)\,d\vartheta\right\} = t + k_2, \quad \text{(B-23)}$$

$$\frac{\sqrt{2}\,GM_{tot}}{\sqrt{k_1^3}}\frac{1}{2}\left\{\cot(\vartheta)\csc(\vartheta) + \int \frac{\csc(\vartheta)[\cot(\vartheta)+\csc(\vartheta)]}{\cot(\vartheta)+\csc(\vartheta)}\,d\vartheta\right\} = t + k_2. \quad \text{(B-24)}$$

Introducing the variable

$$u = \cot(\vartheta) + \csc(\vartheta), \quad \text{(B-25)}$$

so that

$$du = [-\csc^2(\vartheta) - \cot(\vartheta)\csc(\vartheta)]d\vartheta = -[\csc^2(\vartheta) + \cot(\vartheta)\csc(\vartheta)]d\vartheta, \quad \text{(B-26)}$$

we can explicit the integral as follows

$$\frac{\sqrt{2}\,GM_{tot}}{\sqrt{k_1^3}}\frac{1}{2}\left\{\cot(\vartheta)\csc(\vartheta) + \int \frac{[\csc^2(\vartheta)+\cot(\vartheta)\csc(\vartheta)]}{u}\frac{du}{-[\csc^2(\vartheta)+\cot(\vartheta)\csc(\vartheta)]}\right\} = t + k_2, \quad \text{(B-27)}$$

$$\frac{\sqrt{2}\,GM_{tot}}{\sqrt{k_1^3}}\frac{1}{2}\left\{\cot(\vartheta)\csc(\vartheta) - \int \frac{du}{u}\right\} = t + k_2, \quad \text{(B-28)}$$

$$\frac{\sqrt{2}\,GM_{tot}}{\sqrt{k_1^3}}\frac{1}{2}\{\cot(\vartheta)\csc(\vartheta) - \log(u)\} = t + k_2. \quad \text{(B-29)}$$

Substituting back the expression of u from Equation (B-25), we obtain

$$\frac{\sqrt{2}\,GM_{tot}}{\sqrt{k_1^3}}\frac{1}{2}\{\cot(\vartheta)\csc(\vartheta) - \log[\cot(\vartheta) + \csc(\vartheta)]\} = t + k_2. \quad \text{(B-30)}$$

Moreover, substituting back also the expression of ϑ from Equation (B-12), we can write that

$$\vartheta = \sec^{-1}\left[\frac{\sqrt{2\left(\frac{GM_{tot}}{r}+k_1\right)}}{\sqrt{2k_1}}\right] = \sec^{-1}\left(\sqrt{\frac{\frac{GM_{tot}}{r}+k_1}{k_1}}\right), \quad \text{(B-31)}$$

which leads to

$$\frac{\sqrt{2}\,GM_{tot}}{\sqrt{k_1^3}}\frac{1}{2}\left\{\cot\left[\sec^{-1}\left(\sqrt{\frac{\frac{GM_{tot}}{r}+k_1}{k_1}}\right)\right]\csc\left[\sec^{-1}\left(\sqrt{\frac{\frac{GM_{tot}}{r}+k_1}{k_1}}\right)\right] - \log\left[\cot\left[\sec^{-1}\left(\sqrt{\frac{\frac{GM_{tot}}{r}+k_1}{k_1}}\right)\right] + \csc\left[\sec^{-1}\left(\sqrt{\frac{\frac{GM_{tot}}{r}+k_1}{k_1}}\right)\right]\right]\right\}. = t + k_2 \quad \text{(B-32)}$$

However, we can simplify the expression due to the trig-

onometric functions in the general variable x as follows

$$\cot[\sec^{-1}(x)] = \frac{1}{x\sqrt{1-\frac{1}{x^2}}}, \quad \text{(B-33)}$$

as well as

$$\csc[\sec^{-1}(x)] = \frac{1}{\sqrt{1-\frac{1}{x^2}}}. \quad \text{(B-34)}$$

Thus,

$$\frac{\sqrt{2}\,GM_{tot}}{\sqrt{k_1^3}}\frac{1}{2}\left\{\frac{1}{\sqrt{\frac{\frac{GM_{tot}}{r}+k_1}{k_1}}\sqrt{1-\frac{1}{\frac{\frac{GM_{tot}}{r}+k_1}{k_1}}}}\frac{1}{\sqrt{1-\frac{1}{\frac{\frac{GM_{tot}}{r}+k_1}{k_1}}}}-\log\left[\frac{1}{\sqrt{\frac{\frac{GM_{tot}}{r}+k_1}{k_1}}\sqrt{1-\frac{1}{\frac{\frac{GM_{tot}}{r}+k_1}{k_1}}}}+\frac{1}{\sqrt{1-\frac{1}{\frac{\frac{GM_{tot}}{r}+k_1}{k_1}}}}\right]\right\} = t + k_2. \quad \text{(B-35)}$$

Appendix C

$$\frac{\sqrt{2}\,GM_{tot}}{\sqrt{k_1^3}}\frac{1}{2}\left\{\frac{1}{\sqrt{\frac{\frac{GM_{tot}}{r}+k_1}{k_1}}}\frac{1}{\sqrt{1-\frac{1}{\frac{\frac{GM_{tot}}{r}+k_1}{k_1}}}}-\log\left[\frac{1+\sqrt{\frac{\frac{GM_{tot}}{r}+k_1}{k_1}}}{\sqrt{\frac{\frac{GM_{tot}}{r}+k_1}{k_1}}\sqrt{1-\frac{1}{\frac{\frac{GM_{tot}}{r}+k_1}{k_1}}}}\right]\right\} = t + k_2, \quad \text{(C-1)}$$

$$\frac{\sqrt{2}\,GM_{tot}}{\sqrt{k_1^3}}\frac{1}{2}\left\{\frac{1}{\sqrt{\frac{\frac{GM_{tot}}{r}+k_1}{k_1}}}\frac{\frac{GM_{tot}}{r}+k_1}{\frac{GM_{tot}}{r}}-\log\left[\frac{1+\sqrt{\frac{\frac{GM_{tot}}{r}+k_1}{k_1}}}{\sqrt{\frac{\frac{GM_{tot}}{r}+k_1}{k_1}}\sqrt{\frac{\frac{GM_{tot}}{r}}{\frac{GM_{tot}}{r}+k_1}}}}\right]\right\} = t + k_2, \quad \text{(C-2)}$$

$$\frac{\sqrt{2}\,GM_{tot}}{\sqrt{k_1^3}}\frac{1}{2}\left\{\frac{1}{\sqrt{\frac{\frac{GM_{tot}}{r}+k_1}{k_1}}}\frac{\frac{GM_{tot}}{r}+k_1}{\frac{GM_{tot}}{r}}-\log\left[\frac{1+\sqrt{\frac{\frac{GM_{tot}}{r}+k_1}{k_1}}}{\sqrt{\frac{\frac{GM_{tot}}{r}+k_1}{k_1}}\sqrt{\frac{\frac{GM_{tot}}{r}}{\frac{GM_{tot}}{r}+k_1}}}}\right]\right\} = t + k_2, \quad \text{(C-3)}$$

$$\frac{\sqrt{2}\,GM_{tot}}{\sqrt{k_1^3}}\frac{1}{2}\left\{\sqrt{k_1}\frac{\sqrt{\frac{GM_{tot}}{r}+k_1}}{\frac{GM_{tot}}{r}}-\log\left[\frac{\sqrt{k_1}+\sqrt{\frac{GM_{tot}}{r}+k_1}}{\sqrt{\frac{GM_{tot}}{r}}}\right]\right\} = t + k_2, \quad \text{(C-4)}$$

$$\frac{\sqrt{2}\,GM_{tot}}{\sqrt{k_1^3}}\frac{1}{2}\sqrt{k_1}\frac{\sqrt{\frac{GM_{tot}}{r}+k_1}}{\frac{GM_{tot}}{r}}-\frac{\sqrt{2}\,GM_{tot}}{\sqrt{k_1^3}}\frac{1}{2}\log\left[\frac{\sqrt{k_1}+\sqrt{\frac{GM_{tot}}{r}+k_1}}{\sqrt{\frac{GM_{tot}}{r}}}\right] = t + k_2, \quad \text{(C5)}$$

$$\frac{1}{\sqrt{2}\,k_1}r\sqrt{\frac{GM_{tot}}{r}+k_1}-\frac{GM_{tot}}{\sqrt{2}\sqrt{k_1^3}}\log\left[\frac{\sqrt{k_1}+\sqrt{\frac{GM_{tot}}{r}+k_1}}{\sqrt{\frac{GM_{tot}}{r}}}\right] = t + k_2 \quad \text{(C-6)}$$

For limited values of all involved parameters, the equation is equivalent to introducing the inverse hyperbolic tangent function, so that

$$\frac{1}{\sqrt{2}\,k_1}r\sqrt{\frac{GM_{tot}}{r}+k_1}-\frac{GM_{tot}}{\sqrt{2}\sqrt{k_1^3}}\cdot\tanh^{-1}\left[\sqrt{\frac{\frac{GM_{tot}}{r}+k_1}{k_1}}\right] = t + k_2, \quad \text{(C-7)}$$

$$\frac{r}{k_1}\sqrt{\frac{GM_{tot}}{r}+k_1}-\frac{GM_{tot}}{\sqrt{k_1^3}}\cdot\tanh^{-1}\left[\sqrt{\frac{\frac{GM_{tot}}{r}+k_1}{k_1}}\right] = \sqrt{2}(t + k_2). \quad \text{(C-8)}$$

Appendix D

$$\phi(r,t) = \left\{\frac{r}{k_1}\sqrt{\frac{GM_{tot}}{r}+k_1}-\frac{GM_{tot}}{\sqrt{k_1^3}}\cdot\tanh^{-1}\left[\sqrt{\frac{\frac{GM_{tot}}{r}+k_1}{k_1}}\right]\right\}^2 - \left[\sqrt{2}\,(t + k_2)\right]^2 = 0. \quad \text{(D-1)}$$

$$\lim_{r\to 0}\phi(t) = \left[\frac{GM_{tot}}{\sqrt{k_1^3}}\cdot\frac{-i\,\pi}{2}\right]^2 - 2(T + k_2)^2 = 0, \quad \text{(D-2)}$$

$$\frac{G^2M_{tot}^2}{k_1^3}\cdot\frac{\pi^2}{4} - 2(T + k_2)^2 = 0, \quad \text{(D-3)}$$

$$T = \sqrt{\frac{G^2M_{tot}^2}{k_1^3}\cdot\frac{\pi^2}{8}} - k_2, \quad \text{(D-4)}$$

$$T = \frac{\pi GM_{tot}}{2\sqrt{2k_1^3}} - k_2. \quad \text{(D-5)}$$

Appendix E

$$\frac{d\phi(r,t)}{dt}=\frac{d}{dt}\left\{\left\{\frac{1}{k_1}r\sqrt{\frac{GM_{tot}}{r}+k_1}-\frac{GM_{tot}}{\sqrt{k_1^3}}\cdot\tanh^{-1}\left[\sqrt{\frac{\frac{GM_{tot}}{r}+k_1}{k_1}}\right]\right\}^2-\left[\sqrt{2}\,(t+k_2)\right]^2\right\}=0, \tag{E-1}$$

$$\frac{d\phi(r,t)}{dt}=\frac{d}{dt}\left\{\left\{\frac{1}{k_1}r\sqrt{\frac{GM_{tot}}{r}+k_1}-\frac{GM_{tot}}{\sqrt{k_1^3}}\cdot\tanh^{-1}\left[\sqrt{\frac{\frac{GM_{tot}}{r}+k_1}{k_1}}\right]\right\}^2-2(t+k_2)^2\right\}=0, \tag{E-2}$$

$$2\left\{\frac{1}{k_1}r\sqrt{\frac{GM_{tot}}{r}+k_1}-\frac{GM_{tot}}{\sqrt{k_1^3}}\cdot\tanh^{-1}\left[\sqrt{\frac{\frac{GM_{tot}}{r}+k_1}{k_1}}\right]\right\}\left\{\frac{1}{k_1}r'(t)\sqrt{\frac{GM_{tot}}{r}+k_1}+\frac{1}{k_1}r\frac{\left(-\frac{GM_{tot}}{r^2}\right)}{2\sqrt{\frac{GM_{tot}}{r}+k_1}}r'(t)-\frac{GM_{tot}}{\sqrt{k_1^3}}\frac{1}{1-\frac{\frac{GM_{tot}}{r}+k_1}{k_1}}\frac{1}{\sqrt{k_1}}\frac{\left(-\frac{GM_{tot}}{r^2}\right)}{2\sqrt{\frac{GM_{tot}}{r}+k_1}}r'(t)\right\}=4(t+k_2), \tag{E-3}$$

$$2\left\{\frac{1}{k_1}r\sqrt{\frac{GM_{tot}}{r}+k_1}-\frac{GM_{tot}}{\sqrt{k_1^3}}\cdot\tanh^{-1}\left[\sqrt{\frac{\frac{GM_{tot}}{r}+k_1}{k_1}}\right]\right\}\left\{\frac{1}{k_1}r'(t)\sqrt{\frac{GM_{tot}}{r}+k_1}+\frac{1}{k_1}\frac{\left(-\frac{GM_{tot}}{r}\right)}{2\sqrt{\frac{GM_{tot}}{r}+k_1}}r'(t)-\frac{GM_{tot}}{k_1^2}\frac{1}{1-\frac{GM_{tot}+rk_1}{r\,k_1}}\frac{\left(-\frac{GM_{tot}}{r^2}\right)}{2\sqrt{\frac{GM_{tot}}{r}+k_1}}r'(t)\right\}=4(t+k_2), \tag{E-4}$$

$$2\left\{\frac{1}{k_1}r\sqrt{\frac{GM_{tot}}{r}+k_1}-\frac{GM_{tot}}{\sqrt{k_1^3}}\cdot\tanh^{-1}\left[\sqrt{\frac{\frac{GM_{tot}}{r}+k_1}{k_1}}\right]\right\}\left\{\frac{1}{k_1}r'(t)\sqrt{\frac{GM_{tot}}{r}+k_1}+\frac{1}{k_1}\frac{\left(-\frac{GM_{tot}}{r}\right)}{2\sqrt{\frac{GM_{tot}}{r}+k_1}}r'(t)-\frac{GM_{tot}}{k_1^2}\left(-\frac{rk_1}{GM_{tot}}\right)\frac{\left(-\frac{GM_{tot}}{r^2}\right)}{2\sqrt{\frac{GM_{tot}}{r}+k_1}}r'(t)\right\}=4(t+k_2), \tag{E-5}$$

$$2\left\{\frac{1}{k_1}r\sqrt{\frac{GM_{tot}}{r}+k_1}-\frac{GM_{tot}}{\sqrt{k_1^3}}\cdot\tanh^{-1}\left[\sqrt{\frac{\frac{GM_{tot}}{r}+k_1}{k_1}}\right]\right\}\left\{\frac{1}{k_1}r'(t)\sqrt{\frac{GM_{tot}}{r}+k_1}+\frac{1}{k_1}\frac{\left(-\frac{GM_{tot}}{r}\right)}{2\sqrt{\frac{GM_{tot}}{r}+k_1}}r'(t)+\frac{k_1}{k_1^2}\frac{\left(-\frac{GM_{tot}}{r}\right)}{2\sqrt{\frac{GM_{tot}}{r}+k_1}}r'(t)\right\}=4(t+k_2), \tag{E-6}$$

$$2\,r'(t)\left\{\frac{1}{k_1}r\sqrt{\frac{GM_{tot}}{r}+k_1}-\frac{GM_{tot}}{\sqrt{k_1^3}}\cdot\tanh^{-1}\left[\sqrt{\frac{\frac{GM_{tot}}{r}+k_1}{k_1}}\right]\right\}\left\{\frac{\sqrt{\frac{GM_{tot}}{r}+k_1}-\frac{GM_{tot}}{2r\sqrt{\frac{GM_{tot}}{r}+k_1}}}{k_1}-\frac{GM_{tot}}{k_1}\frac{1}{2r\sqrt{\frac{GM_{tot}}{r}+k_1}}\right\}=4(t+k_2), \tag{E-7}$$

$$2\,r'(t)\left\{\frac{1}{k_1}r\sqrt{\frac{GM_{tot}}{r}+k_1}-\frac{GM_{tot}}{\sqrt{k_1^3}}\cdot\tanh^{-1}\left[\sqrt{\frac{\frac{GM_{tot}}{r}+k_1}{k_1}}\right]\right\}\left\{\frac{2r\left(\frac{GM_{tot}}{r}+k_1\right)-GM_{tot}}{2r\,k_1\sqrt{\frac{GM_{tot}}{r}+k_1}}-\frac{GM_{tot}}{2rk_1\sqrt{\frac{GM_{tot}}{r}+k_1}}\right\}=4(t+k_2), \tag{E-8}$$

$$2\,r'(t)\left\{\frac{1}{k_1}r\sqrt{\frac{GM_{tot}}{r}+k_1}-\frac{GM_{tot}}{\sqrt{k_1^3}}\cdot\tanh^{-1}\left[\sqrt{\frac{\frac{GM_{tot}}{r}+k_1}{k_1}}\right]\right\}\left\{\frac{2r\left(\frac{GM_{tot}}{r}+k_1\right)-GM_{tot}-GM_{tot}}{2r\,k_1\sqrt{\frac{GM_{tot}}{r}+k_1}}\right\}=4(t+k_2), \tag{E-9}$$

$$2\,r'(t)\left\{\frac{1}{k_1}r\sqrt{\frac{GM_{tot}}{r}+k_1}-\frac{GM_{tot}}{\sqrt{k_1^3}}\cdot\tanh^{-1}\left[\sqrt{\frac{\frac{GM_{tot}}{r}+k_1}{k_1}}\right]\right\}\left\{\frac{2GM_{tot}+2rk_1-2GM_{tot}}{2r\,k_1\sqrt{\frac{GM_{tot}}{r}+k_1}}\right\}=4(t+k_2), \tag{E-10}$$

$$2\,r'(t)\left\{\frac{1}{k_1}r\sqrt{\frac{GM_{tot}}{r}+k_1}-\frac{GM_{tot}}{\sqrt{k_1^3}}\cdot\tanh^{-1}\left[\sqrt{\frac{\frac{GM_{tot}}{r}+k_1}{k_1}}\right]\right\}\left\{\frac{2rk_1}{2rk_1\sqrt{\frac{GM_{tot}}{r}+k_1}}\right\}=4(t+k_2), \tag{E-11}$$

$$2\,r'(t)\left\{\frac{1}{k_1}r\sqrt{\frac{GM_{tot}}{r}+k_1}-\frac{GM_{tot}}{\sqrt{k_1^3}}\cdot\tanh^{-1}\left[\sqrt{\frac{\frac{GM_{tot}}{r}+k_1}{k_1}}\right]\right\}\left\{\frac{1}{\sqrt{\frac{GM_{tot}}{r}+k_1}}\right\}=4(t+k_2), \tag{E-12}$$

$$r'(t)=\frac{4(t+k_2)\sqrt{\frac{GM_{tot}}{r}+k_1}}{2\left\{\frac{1}{k_1}r\sqrt{\frac{GM_{tot}}{r}+k_1}-\frac{GM_{tot}}{\sqrt{k_1^3}}\cdot\tanh^{-1}\left[\sqrt{\frac{\frac{GM_{tot}}{r}+k_1}{k_1}}\right]\right\}}, \tag{E-13}$$

$$r'(t)=\frac{2\sqrt{k_1^3}(t+k_2)\sqrt{\frac{GM_{tot}}{r}+k_1}}{r\sqrt{k_1}\sqrt{\frac{GM_{tot}}{r}+k_1}-GM_{tot}\cdot\tanh^{-1}\left[\sqrt{\frac{\frac{GM_{tot}}{r}+k_1}{k_1}}\right]}. \tag{E-14}$$

Appendix F

$$\frac{d_{M31}}{k_1}\sqrt{\frac{GM_{tot}}{d_{M31}}+k_1}-\frac{GM_{tot}}{\sqrt{k_1^3}}\cdot\tanh^{-1}\left[\sqrt{\frac{\frac{GM_{tot}}{d_{M31}}+k_1}{k_1}}\right]=\sqrt{2}\,\frac{v_0\left\{d_{M31}\sqrt{k_1}\sqrt{\frac{GM_{tot}}{d_{M31}}+k_1}-GM_{tot}\cdot\tanh^{-1}\left[\sqrt{\frac{\frac{GM_{tot}}{d_{M31}}+k_1}{k_1}}\right]\right\}}{2\sqrt{k_1^3}\sqrt{\frac{GM_{tot}}{d_{M31}}+k_1}}, \tag{F-1}$$

$$\frac{d_{M31}}{k_1}\sqrt{\frac{GM_{tot}}{d_{M31}}+k_1}-\frac{GM_{tot}}{\sqrt{k_1^3}}\cdot\tanh^{-1}\left[\sqrt{\frac{\frac{GM_{tot}}{d_{M31}}+k_1}{k_1}}\right]=\frac{v_0 d_{M31}}{\sqrt{2}\,k_1}-\frac{v_0}{\sqrt{2k_1^3}}\frac{GM_{tot}}{\sqrt{\frac{GM_{tot}}{d_{M31}}+k_1}}\cdot\tanh^{-1}\left[\sqrt{\frac{\frac{GM_{tot}}{d_{M31}}+k_1}{k_1}}\right], \tag{F-2}$$

$$\frac{d_{M31}}{k_1}\left(\sqrt{\frac{GM_{tot}}{d_{M31}}+k_1}-\frac{v_0}{\sqrt{2}}\right)=\frac{GM_{tot}}{\sqrt{k_1^3}}\cdot\tanh^{-1}\left[\sqrt{\frac{\frac{GM_{tot}}{d_{M31}}+k_1}{k_1}}\right]\left(1-\frac{v_0}{\sqrt{2}\sqrt{\frac{GM_{tot}}{d_{M31}}+k_1}}\right). \tag{F-3}$$

Appendix G

$$1-\frac{v_0}{\sqrt{2}\sqrt{\frac{GM_{tot}}{d_{M31}}+k_1}}=0, \tag{G-1}$$

$$v_0=\sqrt{2}\sqrt{\frac{GM_{tot}}{d_{M31}}+k_1}, \tag{G-2}$$

$$v_0^2=2\left(\frac{GM_{tot}}{d_{M31}}+k_1\right), \tag{G-3}$$

$$k_1=\frac{v_0^2}{2}-\frac{GM_{tot}}{d_{M31}}. \tag{G-4}$$

Appendix H

$$k_2=\frac{v_0\left\{d_{M31}\sqrt{\frac{v_0^2}{2}-\frac{GM_{tot}}{d_{M31}}}_1\sqrt{\frac{GM_{tot}}{d_{M31}}+\frac{v_0^2}{2}-\frac{GM_{tot}}{d_{M31}}}-GM_{tot}\cdot\tanh^{-1}\left[\sqrt{\frac{\frac{GM_{tot}}{d_{M31}}+\frac{v_0^2}{2}-\frac{GM_{tot}}{d_{M31}}}{\frac{v_0^2}{2}-\frac{GM_{tot}}{d_{M31}}}}\right]\right\}}{2\sqrt{\left(\frac{v_0^2}{2}-\frac{GM_{tot}}{d_{M31}}\right)^3}\sqrt{\frac{GM_{tot}}{d_{M31}}+\frac{v_0^2}{2}-\frac{GM_{tot}}{d_{M31}}}}, \tag{H-1}$$

$$k_2 = \frac{v_0\left\{d_{M31}\frac{v_0}{\sqrt{2}}\sqrt{\frac{v_0^2}{2}-\frac{GM_{tot}}{d_{M31}}} - GM_{tot}\cdot\tanh^{-1}\left(\frac{v_0}{\sqrt{2}\sqrt{\frac{v_0^2}{2}-\frac{GM_{tot}}{d_{M31}}}}\right)\right\}}{2\frac{v_0}{\sqrt{2}}\sqrt{\left(\frac{v_0^2}{2}-\frac{GM_{tot}}{d_{M31}}\right)^3}}, \tag{H-2}$$

$$k_2 = \frac{v_0\, d_{M31}\frac{v_0}{\sqrt{2}}\sqrt{\frac{v_0^2}{2}-\frac{GM_{tot}}{d_{M31}}}}{2\frac{v_0}{\sqrt{2}}\sqrt{\left(\frac{v_0^2}{2}-\frac{GM_{tot}}{d_{M31}}\right)^3}} - \frac{GM_{tot}v_0\cdot\tanh^{-1}\left(\frac{v_0}{\sqrt{2}\sqrt{\frac{v_0^2}{2}-\frac{GM_{tot}}{d_{M31}}}}\right)}{2\frac{v_0}{\sqrt{2}}\sqrt{\left(\frac{v_0^2}{2}-\frac{GM_{tot}}{d_{M31}}\right)^3}}, \tag{H-3}$$

$$k_2 = \frac{v_0 d_{M31}}{2\left(\frac{v_0^2}{2}-\frac{GM_{tot}}{d_{M31}}\right)} - \frac{GM_{tot}}{\sqrt{2\left(\frac{v_0^2}{2}-\frac{GM_{tot}}{d_{M31}}\right)^3}}\cdot\tanh^{-1}\left(\frac{v_0}{\sqrt{2\left(\frac{v_0^2}{2}-\frac{GM_{tot}}{d_{M31}}\right)}}\right). \tag{H-4}$$

Appendix I

In this part, we resume Ashmore's NTL physics published in several papers. NTL has a good match to observational data and it is basically a multiple interaction process between photons and crystallized electrons through the IGM [37, 42]. At each electron transit the wavelength increases or rather the photon shows up a redshift. Accordingly, the crystallized electron gains this lost energy by means a recoil performing a Simple Harmonic Motion (SHM). By defining λ the incoming photon wavelength and its energy E_λ, we can write the following equilibrium

$$\frac{E_\lambda}{m_e c^2} = \frac{h^2c^2}{\lambda^2 c^2 m_e^2} = \frac{h^2}{\lambda^2 m_e^2}. \tag{I-1}$$

After several algebraic steps contained in the NTL papers, by knowing that the emitted photon has energy $E_{\lambda'}$ and wavelength λ', we obtain that

$$\frac{hc}{\lambda} - \frac{hc}{\lambda'} = \frac{h^2}{\lambda^2 m_e^2}. \tag{I-2}$$

In a classical approach, this equation furtherly reduces to a constant value by imposing that $h \ll \lambda m_e c$ for all incoming wavelengths of the photons $\lambda \gg 10^{11}\ m$

$$\delta\lambda = \frac{h}{m_e c} = 2.43\cdot 10^{-12}\ m. \tag{I-3}$$

It is responsible for the photon loss of energy at each electron transit in the IGM. Moreover, the photon-electron collision cross-section assumes a specific expression [43-45] in the NTL approach based on the interaction of low energy X-rays with matter

$$\sigma = 2r_e\lambda. \tag{I-4}$$

Considering the photon loss of energy applied to N multiple interactions with crystallized electrons in space, we can measure the distance travelled by the photons as the sum of all free mean paths

$$d = \frac{1}{2r_e n_e\left\{\int_0^{N-1}\left[\lambda + x\left(\frac{h}{m_e c}\right)\right]dx\right\}}. \tag{I-5}$$

Introducing the total increase in wavelength as

$$\Delta\lambda = N\delta\lambda, \tag{I-6}$$

Equation (16) leads to

$$z = e^{\frac{H_{NTL}d}{c}} - 1, \tag{I-7}$$

where the Hubble constant is no more related to an expanding space but rather to a photon energy loss parameter in the IGM.

$$H_{NTL} = \frac{2hr_e n_e}{m_e} = 2.05\cdot 10^{-18}\ \frac{1}{sec} = 63.26\,\frac{Km}{\sec Mpc}, \tag{I-8}$$

r_e is the classical electron radius, the electron number density in the IGM is $n_e = 0.5\ el/m^3$ [38], the electron mass m_e and the Planck constant is h. As mentioned, electrons will arrange themselves into a crystal lattice according to Wigner's investigations [33, 34] which introduce for the first time a new quantum aspect for the electrons. Nowadays, Wigner's crystallization has been confirmed in the laboratory [46, 47]. We apply this physics background to the cosmological travel of the photons through the IGM for the description of the redshift mechanism given by the absorption, re-emission and recoiling of the electron-crystal within the electron-crystal lattice or grid in its whole. In order to crystallize on a BBC crystal-lattice the following condition has to be verified [35, 36]:

$$\Gamma \sim \frac{E_{Coul}}{E_{kin}} \geq 175, \tag{I-9}$$

where Γ is the ratio between coulomb potential energy, depending on the electron number density, to the electron kinetic energy function of the temperature. Therefore, electrons can crystallize both a cryogenic temperature and at higher temperature as long as this condition is verified. A point of strength of the theory is that we detect no scattering or blurring of the image as photons travel on a straight line during the cosmological journey through electron crystals. Not by chance, observations do not detect blurred imaging excluding therefore, for instance, a Compton scattering involved in the cosmological redshift process.

References

[1] T. J. Cox & A. Loeb, 2008, The collision between the Milky Way and Andromeda, MNRAS, 386, 1, 461–474. https://doi.org/10.1111/j.1365-2966.2008.13048.x

[2] Cowen, R., 2012, Andromeda on collision course with the Milky Way. Nature. https://doi.org/10.1038/nature.2012.10765

[3] P. J. E. Peebles et al. 2001 Radial and Transverse Velocities of Nearby Galaxies ApJ 554 104. https://doi.org/10.1086/321326

[4] J.-B. Salomon et al. 2016, The transverse velocity of the Andromeda system, derived from the M31 satellite population, MNRAS, 456, 4, 11 4432–4440. https://doi.org/10.1093/mnras/stv2865

[5] E. Carlesi et al., 2016, The tangential velocity of M31: CLUES from constrained simulations, MNRAS Letters, 460, 1, L5–L9. https://doi.org/10.1093/mnrasl/slw059

[6] Sawala et al., 2024, Apocalypse When? No Certainty of a Milky Way - Andromeda Collision. Preprint https://doi.org/10.48550/arXiv.2408.00064

[7] Schiavi R et al., 2019, The collision between the Milky Way and Andromeda and the fate of their Supermassive Black Holes. Proceedings of IAU.; 14(S351): 161-164. https://doi.org/10.1017/S1743921319007439

[8] D. Benisty, 2021, Timing argument take on the Milky Way and Andromeda past encounter A&A, 656, A129. https://doi.org/10.1051/0004-6361/202142096population

[9] C. Scannapieco et al. 2015, The Milky Way and Andromeda galaxies in a constrained hydrodynamical simulation: morphological evolution. A&A, 577, A3. https://doi.org/10.1051/0004-6361/201425494

[10] Roeland P. van der Marel et al 2012 The M31 Velocity Vector. III. future Milky Way M31–M33 orbital evolution, merging, and fate of the Sun ApJ 753 9. https://doi.org/10.1088/0004-637X/753/1/9

[11] Newton, I., 1686, Philosophiae Naturalis Principia Mathematica. London Reg. Soc. Praeses. https://archive.org/details/philosophiaenatu00newt_0

[12] Kepler, J., Brahe, T., and Rudolf II, 1609, Astronomia nova. Heidelberg: G. Voegelinus. https://www.db-thueringen.de/receive/dbt_mods_00052952

[13] L. L. Watkins et al. 2010, The masses of the Milky Way and Andromeda galaxies, MNRAS, 406, 1, 264–278, https://doi.org/10.1111/j.1365-2966.2010.16708.x

[14] Paul J. McMillan, 2017, The mass distribution and gravitational potential of the Milky Way, MNRAS, 465, 1, 76–94. https://doi.org/10.1093/mnras/stw2759

[15] A. G. Riess et al, 2012, Cepheid Period–luminosity Relations In The Near-infrared And The Distance To M31 From The Hubble Space Telescope Wide Field Camera 3* ApJ 745 156. https://doi.org/10.1088/0004-637X/745/2/156

[16] Chandrasekhar, S., 1943, Dynamical Friction. I. General Considerations: the Coefficient of Dynamical Friction, ApJ, 97: 255–262. https://doi.org/10.1086/144517

[17] Chandrasekhar, S., 1943, Dynamical Friction. II. The Rate of Escape of Stars from Clusters and the Evidence for the Operation of Dynamical Friction, ApJ, 97: 263–273. https://doi.org/10.1086/144518

[18] Chandrasekhar, S., 1943, Dynamical Friction. III. a More Exact Theory of the Rate of Escape of Stars from Clusters, ApJ, 98: 54–60. https://doi.org/10.1086/144544

[19] M. J. Rodr ́guez et al., 2020, Hierarchical star formation in nearby galaxies, A&A, 644 A101. https://doi.org/10.1051/0004-6361/202038970

[20] Andrej Prša et al., 2016, Nominal values for selected solar and planetary quantities: IAU 2015 resolution B3 AJ 152 41. https://doi.org/10.3847/0004-6256/152/2/41

[21] R. P. Gupta, 2024, Testing CCC+TL Cosmology with Observed Baryon Acoustic Oscillation Features, ApJ 964 5. https://doi.org/10.3847/1538-4357/ad1bc6

[22] T. Mistele et al., 2024, Indefinitely Flat Circular Velocities and the Baryonic Tully–Fisher Relation from Weak Lensing The ApJ Letters, 969, 1. https://doi.org/10.3847/2041-8213/ad54b0

[23] Trinchera A., 2023, Cosmological redshift and Hubble tension explained by means of the FLRWT time-metric framework and transit physics in the IGM. Front. Astron. Space Sci. 9: 1014433. https://doi.org/10.3389/fspas.2022.1014433

[24] R. P. Gupta, 2023, JWST early Universe observations and ΛCDM cosmology, MNRAS, 524, 3, 3385–3395. https://doi.org/10.1093/mnras/stad2032

[25] Vicki Kuhn et al., 2024, JWST Reveals a Surprisingly High Fraction of Galaxies Being Spiral-like at $0.5 \leq z \leq 4$ ApJL 968 L15. https://doi.org/10.3847/2041-8213/ad43eb

[26] Haojing Yan et al., 2023, First Batch of $z \approx 11$–20 Candidate Objects Revealed by the James Webb Space Telescope Early Release Observations on SMACS 0723-73 ApJL 942 L9. https://doi.org/10.3847/2041-8213/aca80c

[27] Ashmore, L. E., 2019, Calculating the redshifts of distant galaxies from first principles by the new tired light theory (NTL). J. Phys. Conf. Ser. 1251, 012007. https://doi.org/10.1088/1742-6596/1251/1/012007

[28] Nernst, W., 1938, Weitere Prüfung der Annahme eines stationären Zustandes im Weltall. Z. Phys. 106, 633–661. https://doi.org/10.1007/BF01339902

[29] Zwicky, F., 1929, On the redshift of spectral lines through interstellar space. PNAS 15, 773–779. https://doi.org/10.1073/pnas.15.10.773

[30] Pecker, J.-C., and Vigier, J.-P., 1987, A possible tired-light mechanism, IAU symposia Beijing. 507–511. https://doi.org/10.1007/978-94-009-3853-3_48

[31] Arp, H. C., 1990, Comments on tired-light mechanisms. IEEE Trans. Pl. Sci. 18(1), 77. https://doi.org/10.1109/27.45508

[32] LaViolette, P. A., 1986, Is the Universe Really Expanding? ApJ, 301, 544-553. https://doi.org/10.1086/163922

[33] Wigner E. P., 1934, On the Interaction of Electrons in Metals; Physical Review 46 1002. https://doi.org/10.1103/PhysRev.46.1002

[34] Wigner E. P., 1938, Effects of the Electron Interaction on the Energy Levels of Electrons in Metals. Trans. Faraday Soc. 34, 678. https://doi.org/10.1007/978-3-642-59033-7_42

[35] E. L. Pollock & J. P. Hansen, 1973, Statistical mechanics of dense ionized matter. II. Equilibrium properties and melting transition of the crystallized one-component plasma, Phys. Rev. A 8 3110–3122. http://dx.doi.org/10.1103/%20PhysRevA.8.3110

[36] W. L. Slattery et al., 1980, Improved equation of state for the classical one-component plasma, Phys. Rev. A 21 2087–2095. http://dx.doi.org/10.1103/PhysRevA.21.2087

[37] Ashmore, L. E., 2022, Data from 14, 577 cosmological objects and 14 FRBs confirm the predictions of new tired light (NTL) and lead to a new model of the IGM. J. Phys: Conf. Ser. 2197 012003. https://doi.org/10.1088/1742-6596/2197/1/012003

[38] Ashmore, L., 2024, Data from Twenty-Three FRB's Confirm the Universe Is Static and Not Expanding. JHEPGC, 10, 1152-1177. https://doi.org/10.4236/jhepgc.2024.103070

[39] Trinchera, A., 2021, Redshift Anomaly on the Solar Disk as Multiple Interactions between Photons and Electrons. JHEPGC, 7, 1-51. https://doi.org/10.4236/jhepgc.2021.71001

[40] Trinchera, A., 2021, Redshift Anomaly of the 2292 MHz Radio Signal Emitted by the Pioneer-6 Space Probe as Multiple Interactions with Photo-Ionized Electrons in the Solar Corona. JHEPGC, 7, 1107-1156. https://doi.org/10.4236/jhepgc.2021.73066

[41] Trinchera A., 2022, CMB as thermal radiation from cosmic dust grains in equilibrium with the redshifted starlight J. Phys.: Conf. Ser. 2197 012026. https://doi.org/10.1088/1742-6596/2197/1/012026

[42] Ashmore, L. E., 2019, Galaxies "Boiling off" Electrons Due to the Photo-Electric Effect Leading to a New Model of the IGM and a Possible Mechanism for "Dark Matter". JHEPGC, 5, 181-192. https://doi.org/10.4236/jhepgc.2019.51010

[43] Henke B. L. et al., 1993, X-Ray Interactions: Photoabsorption, Scattering Transmission and Reflection at E = 50 - 30,000 eV Z = 1 – 92. Atomic Data and Nuclear Data Tables 54 p181-342. http://dx.doi.org/10.1006/adnd.1993.1013

[44] Henke B. L. et al., 2001, X-Ray Data Booklet Chapter 1. LBNL/PUB490 Rev. 2 Lawrence Berkeley National Laboratory University of California Berkeley 44-52. https://physics.uwo.ca/~lgonchar/courses/p9826/xdb.pdf#page=

[45] Hubbell J. H. et al., 1975, Atomic Form Factors, Incoherent Scattering Functions, and Photon Cross Sections Journal of Physical and Chemical Reference Data 4 471-538. http://dx.doi.org/10.1063/1.555523

[46] Smoleński, T. et al., 2021, Signatures of Wigner crystal of electrons in a monolayer semiconductor. Nature 595, 53–57. https://doi.org/10.1038/s41586-021-03590-4

[47] Tsui, YC. et al., 2024, Direct observation of a magnetic-field-induced Wigner crystal. Nature 628, 287–292. https://doi.org/10.1038/s41586-024-07212-7

Biography

Alessandro Trinchera is an Italian and German independent tired-light researcher who graduated in Astro & Particle Physics at the renowned University of Tübingen in Germany very close to J. Kepler's birth place. He started theoretical investigations in the Academy during the COVID-19 pandemic. His scientific approach, providing validation to a specific and alternative cosmological methodology, is not in accordance with the fund-based research of the astrophysics departments. He has still been pursuing his work with devotion also due to some important publications drafted alongside his studies as well as his thesis work. His field of interest embraces the interaction between photons and particles in space, the solar and space-probes redshift anomalies as well as the cosmological redshift and its related parameters in a non-expanding framework.